

LIGO-T950005-00-D

LIGO BEAM TUBE STUDY REPORT

(Dynamic Response of the Beam Tube to the
Hanford, WA Site Ambient Vibration Spectrum)

performed as part of the

LIGO Baffle / Scattering Review

by

M. Gamble of the LIGO Detector Group

7 March 1995

LIGO BEAM TUBE STUDY REPORT

(Dynamic Response of the Beam Tube to the Hanford, WA Site Ambient Vibration Spectrum)

Introduction

This analysis was undertaken in support of the LIGO Baffle / Scattering Review held at the California Institute of Technology on January 6 and 7, 1995. This review focused on the optical qualities of the LIGO beam tubes and baffles and their impact on LIGO's overall performance. Calculations estimating LIGO performance parameters had assumed a beam tube free from dynamic responses that would amplify seismic motions introduced to the tube through its support hardware. This report describes "order of magnitude" calculations performed to provide insight into the structural dynamic behavior of the beam tube and its support structure and the dynamic response of the system they compose to random vibrations.

Beam tube structural dynamics calculations were presented during the January review. At the review's conclusion, homework was assigned that lead to improvements in these calculations (more accurate finite element models and results). The following information will be addressed in this report and bears the indicated refinements:

- 3D beam calculations have been improved to account for the weight and possible damping enhancement of a 10-cm-thick layer of external insulation applied to the tube.
- The stiffness properties of the bellows connecting the two sections of tube has been more accurately modeled.
- A 3D shell model of the system was developed to describe the ovalization vibration modes of the system in addition to defining the beam-bending modes described by the 3D beam model.
- Transfer functions and dynamic responses are plotted as absolute quantities.
- Transfer functions of the beam and shell models are expressed as continuous functions of frequency and are compared with a 2D model of the system generated by an independent contractor.
- Structural dynamic response of the models excited by an input power spectrum are expressed as continuous functions of frequency.

Objective

The objective of this analysis was to determine the transfer function matrix elements, expressed as continuous functions of frequency, of the LIGO beam tube and its support hardware and estimate the dynamic response of the tube to the seismic input spectrum characteristic of the Hanford, WA site.

Method

A general purpose finite element code was used to determine the response of tube extension and bending modes (using 3D, kirchoff beam elements) and tube ovalization modes (using thin, isoparametric shell elements) supported by grounded hardware (modeled using 2D spring elements).

Assumptions

The input power spectrum is applied directly to the base nodes of the support elements thereby neglecting the effects of soil and structure interactions. It is assumed that the tube's vibrational behavior can be characterized by modeling only 2 rigid pipe supports and a single guided support encompassing an arbitrary bellows. It is further assumed that small strains and linear/elastic materials characterize the deformations. Finally, it is assumed that the diagonal matrix elements are much larger than the off diagonal elements.

Finite Element Models

Two finite element models were developed to perform the analysis. The model using beam elements to describe the tube possesses hundreds of degrees of freedom (dof's) whereas the shell model of the tube uses more than ten thousand dof's and requires commensurably longer execution time (the order of dof's squared). The beam model is 3 dimensional and well describes the stiffness of the supports in three orthogonal directions but is incapable of describing ovalization or so called "shell" modes of the tube. Solutions of gravitational-induced sag obtained using the beam model were found to agree closely with 2D beam-based finite element calculations performed by an independent contractor. This 3D beam model demonstrated a low frequency mode of vibration, associated with the low transverse stiffness of the guided support, that was not resolved by the contractor's 2D model of the tube and support structure.

Dynamic response estimates for an input consisting of the Hanford, WA vibration spectrum, assuming modal damping of 2% of critical, were calculated using the 3D beam model whereas no responses were generated by the contractor. Neither this initial 3D beam model nor the contractor's 2D model accounted for the weight or possible added damping of the tube's external insulation. A subsequent version of this 3D model was developed and included the increased weight, approximately 22%, and damping, assumed to increase modal damping by a factor of 2 times that of fabricated steel (from 2% to 4% of critical), associated with the insulation. The impact of the addition of the insulation's weight on the dynamic behavior of the system is well known, the increased damping effect of the application of this material is not understood. The system's dynamic response scales linearly with increased damping, however, the performance of the damper is generally a function of frequency and in this case a strong function of the method of application of the insulation material. Whereas a well adhered, low Q damping material could increase the effective modal damping of the tube/insulation system to 10% of critical, because of a lack of detailed information regarding the LIGO scenario a value of 4% was chosen for the analysis. More accurate analytical results would require the generation of effective damping test data for input.

A 3D shell model was developed to accurately describe the ovalization vibration modes of the tube/support structure system. This model also accounted for the weight of the 10-cm-thick layer of insulation and assumed modal damping of 4% of critical.

Results Discussion

The results included in Table 1 present a comparison of calculations performed using the 2D and 3D beam models as well as the 3D shell model. Though the Table bears only a few of the largest transfer function matrix elements expressed as **gains** (simply the dimensionless magnitude of the complex-valued functions evaluated at a particular frequency), plots of the transfer functions of the tube/support system for each of the 3D models are contained in Appendix I. In all cases, the transfer function **plots** express the **squared magnitudes** of the complex-valued transfer functions and are dimensionless quantities expressed as continuous functions of frequency.

Close inspection of the transfer functions of the 3D beam and 3D shell models reveal the fundamental nature of the system. The tube is a very long, slender entity. Such a body can be accurately described as a beam and does not require the more elegant (and computationally intensive) description afforded by a shell representation. This is clear in the fact that the characteristic shapes (spectral behavior) and magnitudes of the transfer functions of the beam and shell models are nearly identical. Were the tube's length short and its inner diameter large, many previously unseen modes having a significant participatory modal mass, and hence large gain, would have been added to the spectrum generated using the beam model. In fact, the first "apparent" true ovalization mode (significant shell behavior in the absence of beam bending) is mode 13 occurring at 45 Hz. This mode is actually a facet of the boundary conditions applied to the model, which could be improved upon if necessary, and is not characteristic of the physically realizable system. Hence, its significant gain should be disregarded. The first true shell mode is mode 17 occurring at 55 Hz which does not exhibit some participatory modal mass, hence has a modest gain associated with it. The same is true for all subsequent shell modes exhibited at higher frequencies and necessarily excited by a rapidly diminishing input spectrum.

Furthermore, the first coupled shell mode (significant ovalization and bending, one full wave of bending, expressed simultaneously) is mode 11 occurring at 40 Hz. The gains of nodes around the girth of the tube at the half-wave point (where ovalization could be somewhat isolated from bending) were compared to the gains of nodes at the quarter points of the body (where bending would produce a maximum for this mode). The modal mass associated with the beam bending behavior of the mode far outstripped that of the ovalization. This comparison further demonstrated that greater energy is associated with the tube's bending vibration modes than its shell modes. The transfer functions and modal plots of the shell model contained in Appendix I clearly indicate that the shell modes of the body have gain associated with them. The accuracy of the model's input, however, is not accurate enough to merit confidence in gain factors of 2x or 3x.

Plots of the mode shapes and dynamic response of the 3D beam model with insulation weight and modal damping of 4%, excited by the LIGO Hanford, WA site input power spectrum, can be found in Appendix I. This is the most reasonable of all cases run. Shell responses are not included for reasons stated above. Furthermore, the units of the response plots found in the Appendix are nonideal---- responses are plotted in power units of **(micro-inches)²/Hz**... It is believed that the transfer functions are the most valuable information produced by this work.

Table I. LIGO Beam Tube Structural Dynamics Analysis Results

	<i>2D Beam Model w/o Insulation $\xi = N/A$</i>	<i>3D Beam Model w/o Insulation $\xi = 0.02$</i>	<i>3D Beam Model with Insulation $\xi = 0.02$</i>	<i>3D Beam Model with Insulation $\xi = 0.04$</i>	<i>3D Shell Model with Insulation $\xi = 0.04$</i>
Maximum Static Deflection (mm)	1.5	1.5	1.8	1.8	1.9
Vibrational Mode		Support	Support	Support	Support
Princ. Direction		Z	Z	Z	Z
Frequency (Hz)		3.2	3.1	3.1	3.0
Gain, node point		32x, n12	36x, n12	17x, n12	19x, n61
Vibrational Mode	0.5 Waves	0.5 Waves	0.5 Waves	0.5 Waves	0.5 Waves
Princ. Direction	Y and Z	Y	Y	Y	Y
Frequency (Hz)	12.5	14	13	13	11.5
Gain, node point	N/A	30x, n19	30x, n19	15x, n19	15x, n1790
Vibrational Mode		Support	Support	Support	Support
Princ. Direction		Z	Z	Z	Z
Frequency (Hz)		18	16.7	16.7	18.5
Gain, node point		15x, n12	15x, n12	8x, n12	6x, n61
Vibrational Mode	1.0 Waves	1.0 Waves	1.0 Waves	1.0 Waves	1.0 Waves
Princ. Direction	Y and Z	Y	Y	Y	Z
Frequency (Hz)	40	43	39	39	40
Gain, node point	N/A	10x, n12	10x, n12	5x, n12	5x, n61
Vibrational Mode		Extension	Extension	Extension	Extension
Princ. Direction		X	X	X	X
Frequency (Hz)		60	55	55	52
Gain, node point		30x, n12	30x, n12	15x, n12	15x, n61
Vibrational Mode	1.5 Waves	1.5 Waves	1.5 Waves	1.5 Waves	1.5 Waves
Princ. Direction	Y and Z	Y	Y	Y	Y
Frequency (Hz)	83	75	69	69	69
Gain, node point	N/A	20x, n19	12x, n19	5x, n19	5x, n1790
Vibrational Mode		Coupled	Coupled	Coupled	Not Calculated
Princ. Direction		X	X	X	
Frequency (Hz)		180	165	165	
Gain, node point		10x, n12	10x, n12	5x, n12	

Note: For the beam models, node 12 is located at the bellows, node 19 is located approximately midway between the bellows and the fixed support, and node 3 is located approximately one quarter of the distance between the bellows and fixed support, measured from the fixed support. For the shell model, nodes 61, 1790, and 117 are analogous to nodes 12, 19, and 3 respectively.

APPENDIX I

General Information

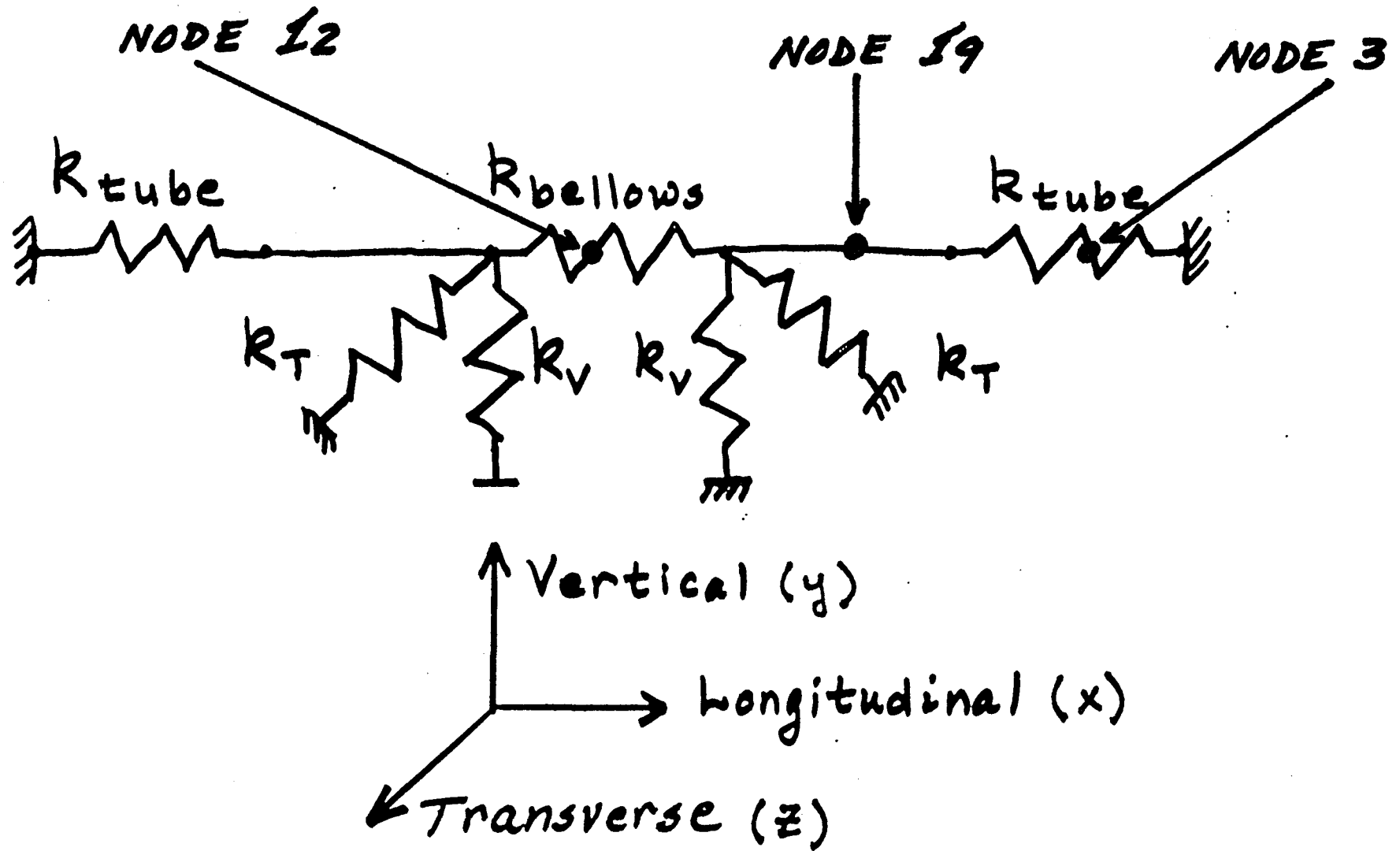
Finite Element Model Schematic

LIGO Input Power Spectra

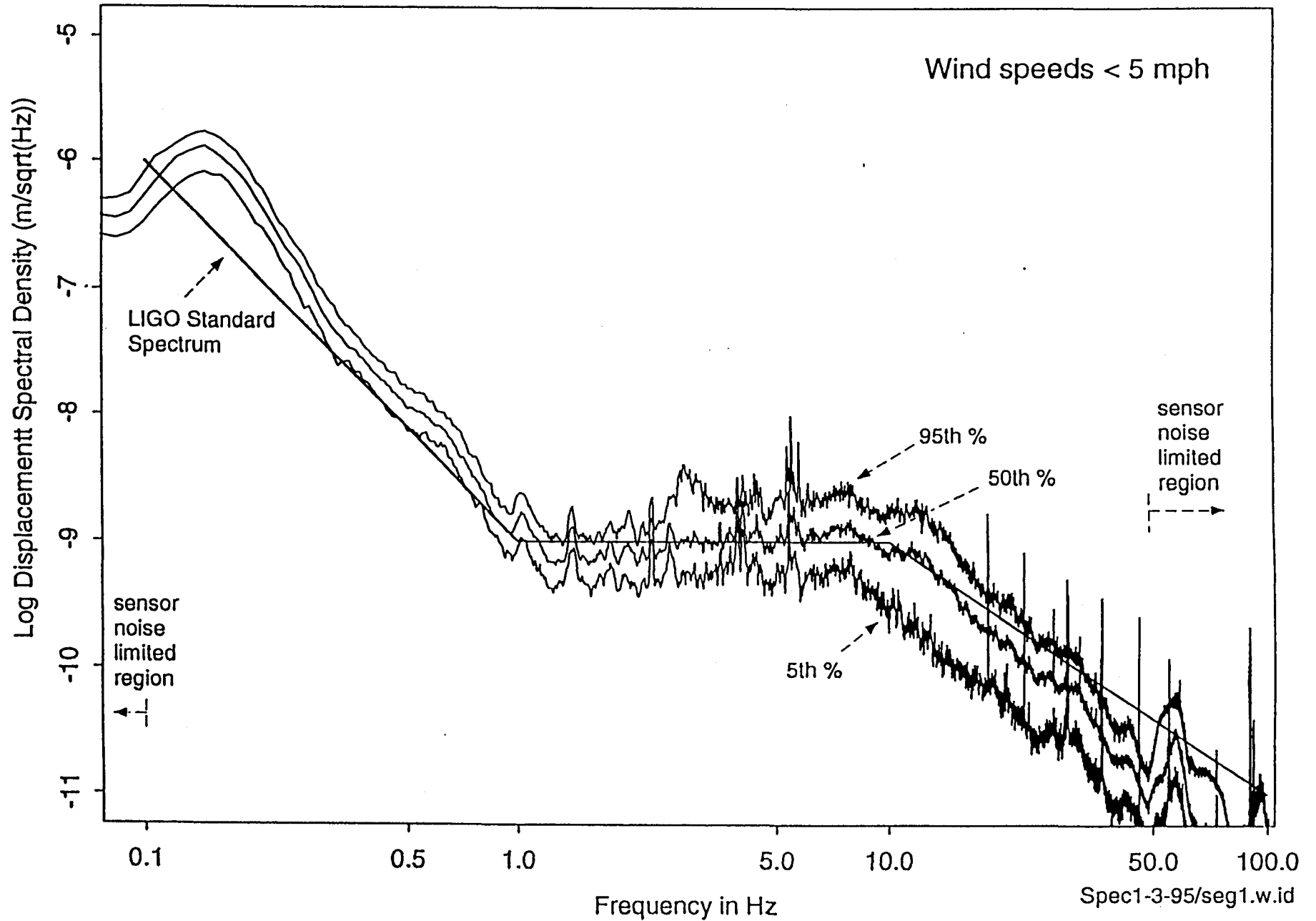
Mechanical Drawings of:

1. Fixed Support
2. Guided Support

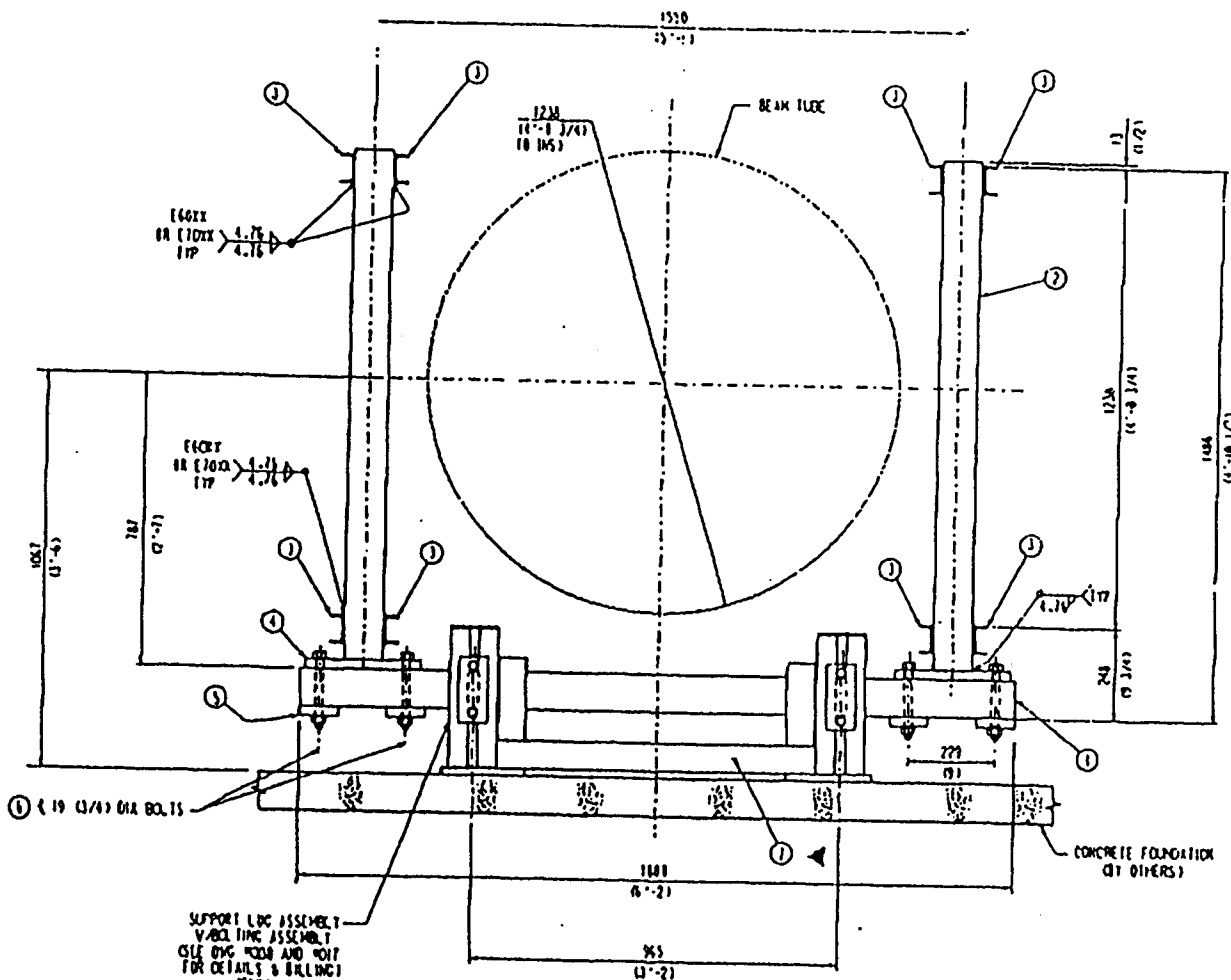
3D Finite Element Model Schematic



Hanford Corner Station SW Arm Axis, Morning Traffic December 13, 1994 (Preliminary Data)



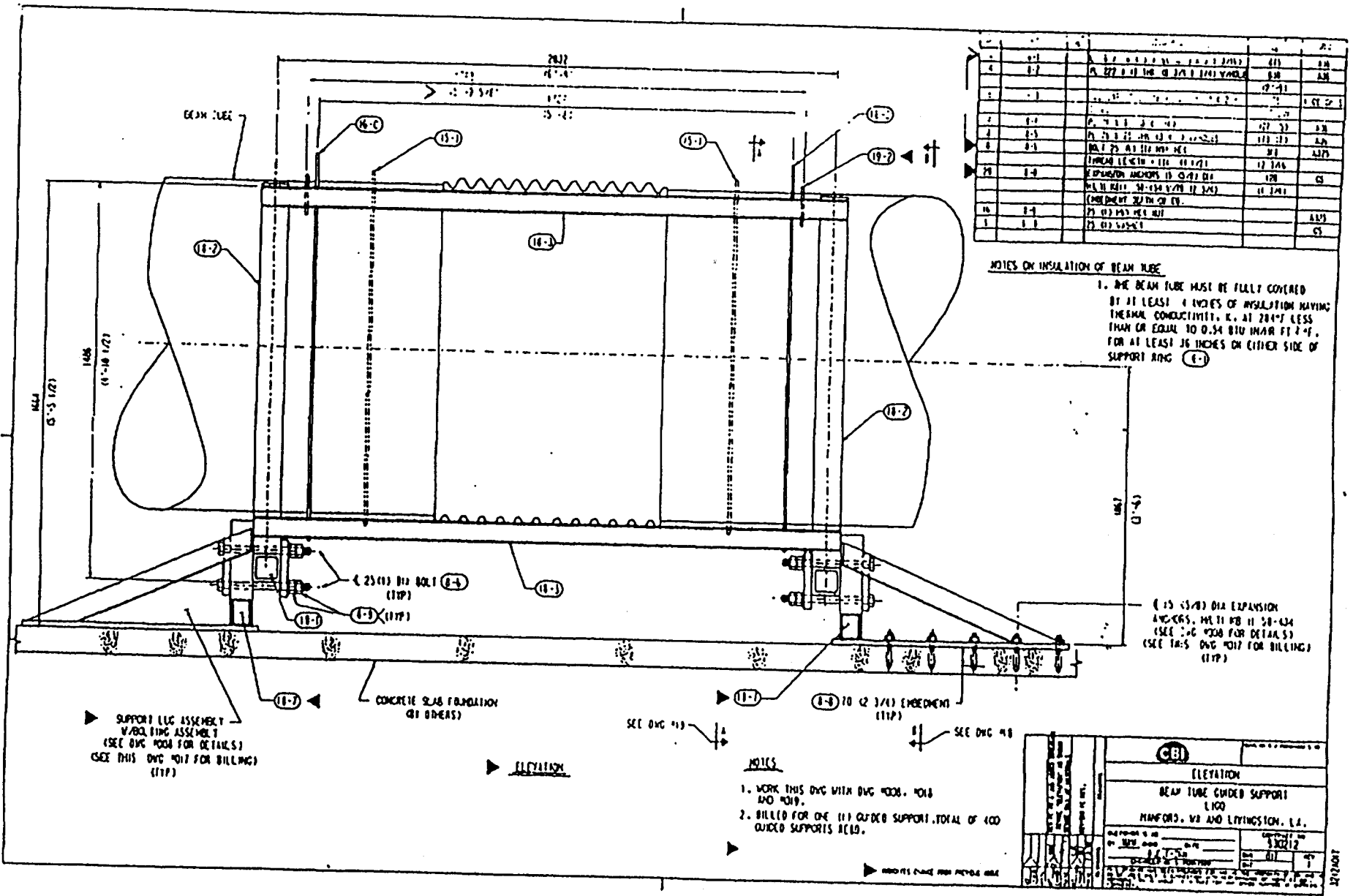
NO.	REV.	DESCRIPTION	DATE	BY
1	0-1	ISSUED FOR BIDDING	08/01/80	W.S.D.
2	0-2	REVISIONS MADE	08/01/80	W.S.D.
3	0-3	REVISIONS MADE	08/01/80	W.S.D.
4	0-4	REVISIONS MADE	08/01/80	W.S.D.
5	0-5	REVISIONS MADE	08/01/80	W.S.D.
6	0-6	REVISIONS MADE	08/01/80	W.S.D.
7	0-7	REVISIONS MADE	08/01/80	W.S.D.
8	0-8	REVISIONS MADE	08/01/80	W.S.D.
9	0-9	REVISIONS MADE	08/01/80	W.S.D.
10	0-10	REVISIONS MADE	08/01/80	W.S.D.
11	0-11	REVISIONS MADE	08/01/80	W.S.D.
12	0-12	REVISIONS MADE	08/01/80	W.S.D.
13	0-13	REVISIONS MADE	08/01/80	W.S.D.
14	0-14	REVISIONS MADE	08/01/80	W.S.D.
15	0-15	REVISIONS MADE	08/01/80	W.S.D.
16	0-16	REVISIONS MADE	08/01/80	W.S.D.
17	0-17	REVISIONS MADE	08/01/80	W.S.D.
18	0-18	REVISIONS MADE	08/01/80	W.S.D.
19	0-19	REVISIONS MADE	08/01/80	W.S.D.
20	0-20	REVISIONS MADE	08/01/80	W.S.D.



SECTION 1-1
 FROM DWG 10111
 (SECTIONS NOT SHOWN FOR CLARITY)

- NOTES**
1. WORK 1-15 DWG WITH DWG 1000, 1017 AND 1019.
 2. BILLED FOR ONE (1) GUIDED SUPPORT. TOTAL OF 400 GUIDED SUPPORTS REQD.

CB	
SECTION DETAILS	
BEAM TUBE GUIDED SUPPORT	
100	
FARMFORD, VA. AND LITTINGSTON, A.A.	
DATE: 08/01/80	BY: W.S.D.
CHECKED: []	DATE: []
APPROVED: []	DATE: []



NO.	REV.	DESCRIPTION	DATE	BY	CHKD.
1	0-1	AS SHOWN			
2	0-2	ADD 18-1 TO 18-4			
3	0-3	ADD 18-5 TO 18-7			
4	0-4	ADD 18-8 TO 18-10			
5	0-5	ADD 18-11 TO 18-13			
6	0-6	ADD 18-14 TO 18-16			
7	0-7	ADD 18-17 TO 18-19			
8	0-8	ADD 18-20 TO 18-22			
9	0-9	ADD 18-23 TO 18-25			
10	0-10	ADD 18-26 TO 18-28			
11	0-11	ADD 18-29 TO 18-31			
12	0-12	ADD 18-32 TO 18-34			
13	0-13	ADD 18-35 TO 18-37			
14	0-14	ADD 18-38 TO 18-40			
15	0-15	ADD 18-41 TO 18-43			
16	0-16	ADD 18-44 TO 18-46			
17	0-17	ADD 18-47 TO 18-49			
18	0-18	ADD 18-50 TO 18-52			
19	0-19	ADD 18-53 TO 18-55			
20	0-20	ADD 18-56 TO 18-58			
21	0-21	ADD 18-59 TO 18-61			
22	0-22	ADD 18-62 TO 18-64			
23	0-23	ADD 18-65 TO 18-67			
24	0-24	ADD 18-68 TO 18-70			
25	0-25	ADD 18-71 TO 18-73			
26	0-26	ADD 18-74 TO 18-76			
27	0-27	ADD 18-77 TO 18-79			
28	0-28	ADD 18-80 TO 18-82			
29	0-29	ADD 18-83 TO 18-85			
30	0-30	ADD 18-86 TO 18-88			
31	0-31	ADD 18-89 TO 18-91			
32	0-32	ADD 18-92 TO 18-94			
33	0-33	ADD 18-95 TO 18-97			
34	0-34	ADD 18-98 TO 18-100			
35	0-35	ADD 18-101 TO 18-103			
36	0-36	ADD 18-104 TO 18-106			
37	0-37	ADD 18-107 TO 18-109			
38	0-38	ADD 18-110 TO 18-112			
39	0-39	ADD 18-113 TO 18-115			
40	0-40	ADD 18-116 TO 18-118			
41	0-41	ADD 18-119 TO 18-121			
42	0-42	ADD 18-122 TO 18-124			
43	0-43	ADD 18-125 TO 18-127			
44	0-44	ADD 18-128 TO 18-130			
45	0-45	ADD 18-131 TO 18-133			
46	0-46	ADD 18-134 TO 18-136			
47	0-47	ADD 18-137 TO 18-139			
48	0-48	ADD 18-140 TO 18-142			
49	0-49	ADD 18-143 TO 18-145			
50	0-50	ADD 18-146 TO 18-148			
51	0-51	ADD 18-149 TO 18-151			
52	0-52	ADD 18-152 TO 18-154			
53	0-53	ADD 18-155 TO 18-157			
54	0-54	ADD 18-158 TO 18-160			
55	0-55	ADD 18-161 TO 18-163			
56	0-56	ADD 18-164 TO 18-166			
57	0-57	ADD 18-167 TO 18-169			
58	0-58	ADD 18-170 TO 18-172			
59	0-59	ADD 18-173 TO 18-175			
60	0-60	ADD 18-176 TO 18-178			
61	0-61	ADD 18-179 TO 18-181			
62	0-62	ADD 18-182 TO 18-184			
63	0-63	ADD 18-185 TO 18-187			
64	0-64	ADD 18-188 TO 18-190			
65	0-65	ADD 18-191 TO 18-193			
66	0-66	ADD 18-194 TO 18-196			
67	0-67	ADD 18-197 TO 18-199			
68	0-68	ADD 18-200 TO 18-202			
69	0-69	ADD 18-203 TO 18-205			
70	0-70	ADD 18-206 TO 18-208			
71	0-71	ADD 18-209 TO 18-211			
72	0-72	ADD 18-212 TO 18-214			
73	0-73	ADD 18-215 TO 18-217			
74	0-74	ADD 18-218 TO 18-220			
75	0-75	ADD 18-221 TO 18-223			
76	0-76	ADD 18-224 TO 18-226			
77	0-77	ADD 18-227 TO 18-229			
78	0-78	ADD 18-230 TO 18-232			
79	0-79	ADD 18-233 TO 18-235			
80	0-80	ADD 18-236 TO 18-238			
81	0-81	ADD 18-239 TO 18-241			
82	0-82	ADD 18-242 TO 18-244			
83	0-83	ADD 18-245 TO 18-247			
84	0-84	ADD 18-248 TO 18-250			
85	0-85	ADD 18-251 TO 18-253			
86	0-86	ADD 18-254 TO 18-256			
87	0-87	ADD 18-257 TO 18-259			
88	0-88	ADD 18-260 TO 18-262			
89	0-89	ADD 18-263 TO 18-265			
90	0-90	ADD 18-266 TO 18-268			
91	0-91	ADD 18-269 TO 18-271			
92	0-92	ADD 18-272 TO 18-274			
93	0-93	ADD 18-275 TO 18-277			
94	0-94	ADD 18-278 TO 18-280			
95	0-95	ADD 18-281 TO 18-283			
96	0-96	ADD 18-284 TO 18-286			
97	0-97	ADD 18-287 TO 18-289			
98	0-98	ADD 18-290 TO 18-292			
99	0-99	ADD 18-293 TO 18-295			
100	0-100	ADD 18-296 TO 18-298			

NOTES ON INSULATION OF BEAM TUBE

1. THE BEAM TUBE MUST BE FULLY COVERED BY AT LEAST 1 INCHES OF INSULATION HAVING THERMAL CONDUCTIVITY, K, AT 284°F LESS THAN OR EQUAL TO 0.54 BTU IN/HR FT² °F, FOR AT LEAST 36 INCHES ON EITHER SIDE OF SUPPORT RING (E).

(E) IS (3/8) DIA EXPANSION ANCHORS, MET 18 11 58-434 (SEE DGC 4000 FOR DETAIL) (SEE THIS DGC 4017 FOR BILLING) (ITP)

▶ SUPPORT ILC ASSEMBLY W/ RING ASSEMBLY (SEE DGC 4004 FOR DETAILS) (SEE THIS DGC 4017 FOR BILLING) (ITP)

▶ **ELEVATION**

SEE DGC 413

SEE DGC 418

NOTES

1. WORK THIS DGC WITH DGC 4000, 4018 AND 4019.
2. BILLED FOR ONE (1) GUIDED SUPPORT, TOTAL OF 400 GUIDED SUPPORTS REQD.

(CBI)	
ELEVATION	
BEAM TUBE GUIDED SUPPORT	
L100	
MANFORD, VA AND LIVINGSTON, L.A.	
DATE: 01/12/82	SCALE: 1/8" = 1'-0"
BY: J. T. SMITH	CHKD: J. T. SMITH
PROJECT: 82-01	REV: 1
DRAWING NO. 82-01-100	

1/27/82

3D Shell Model

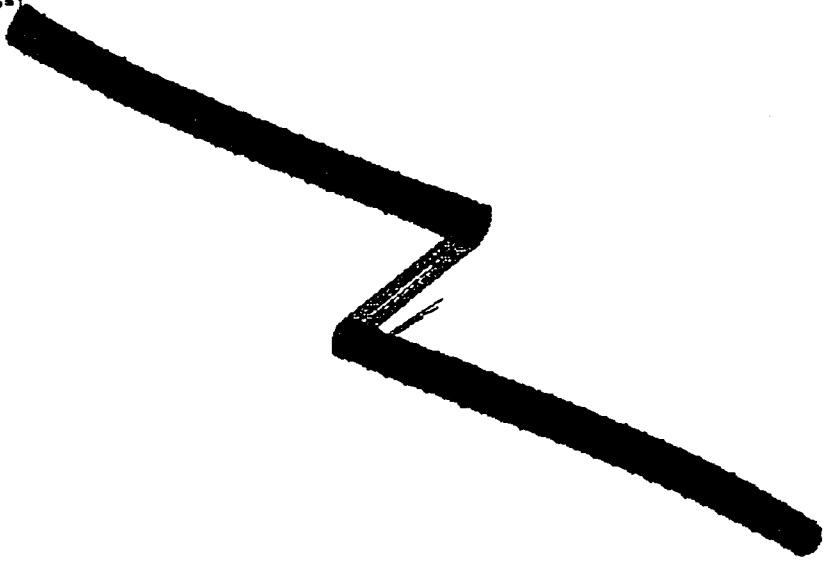
Static, Gravity-Induced Displacement
Natural Frequencies of Vibration
Deformed Mode Shapes

Lin DISP Lc=1

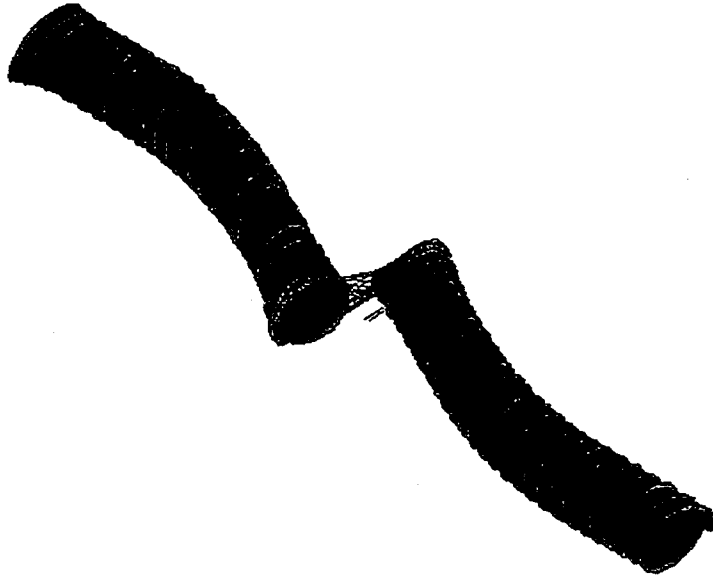
Y - Disp [inches]



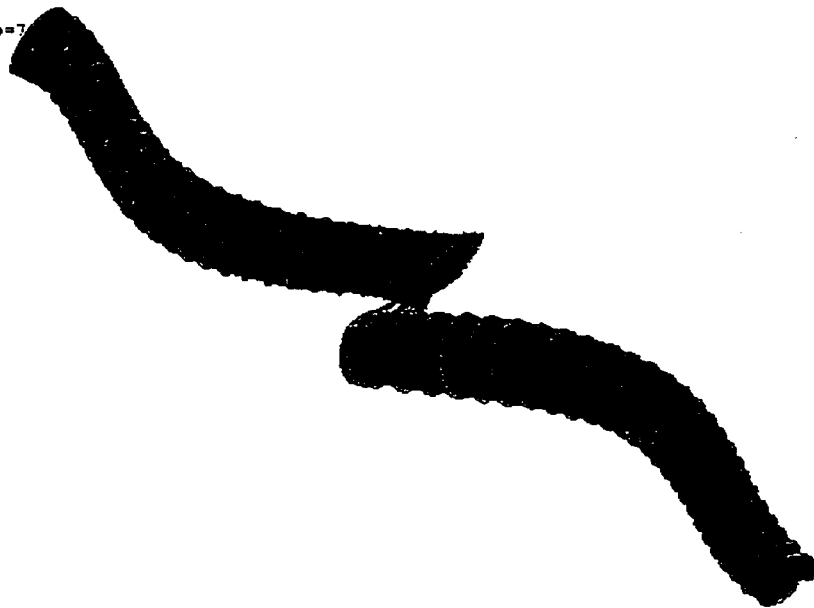
3 Hz F_Mode=1



10.3 Hz F_Mode=3



18.5Hz F_Mode=7

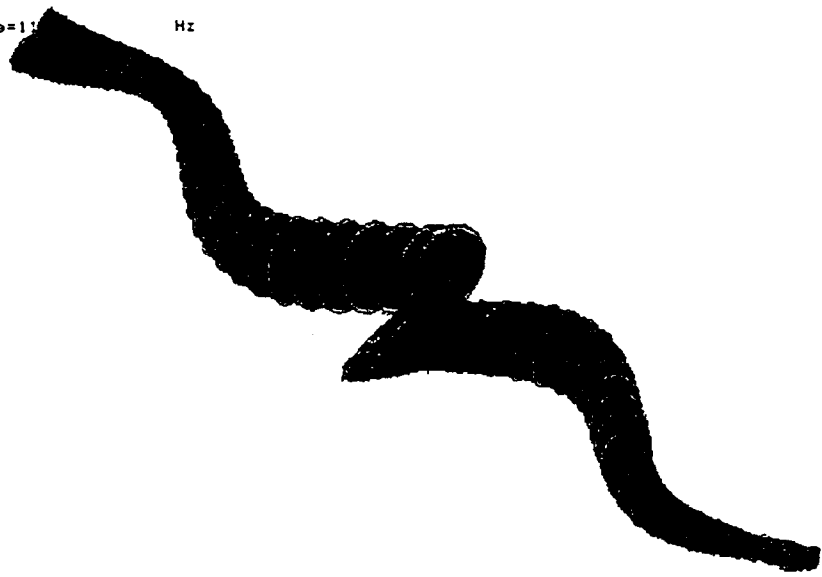


31 Hz F_Mode=9

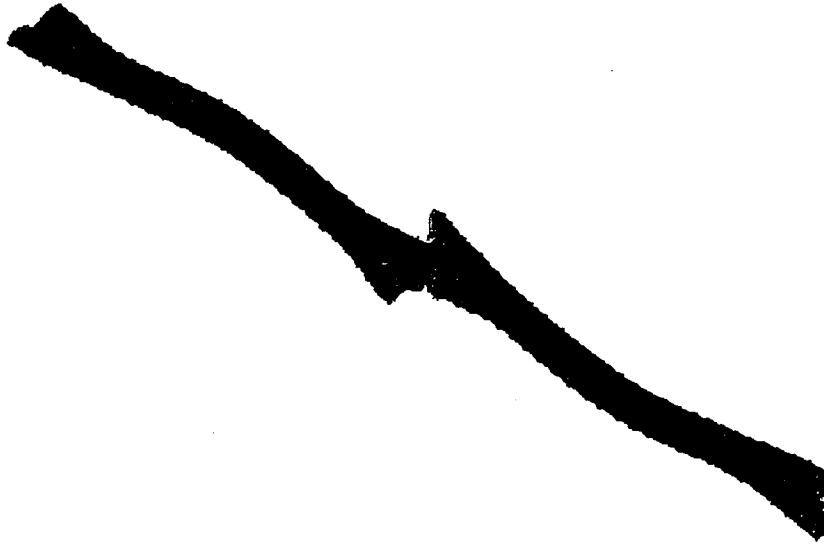


40 Hz F_mode=11

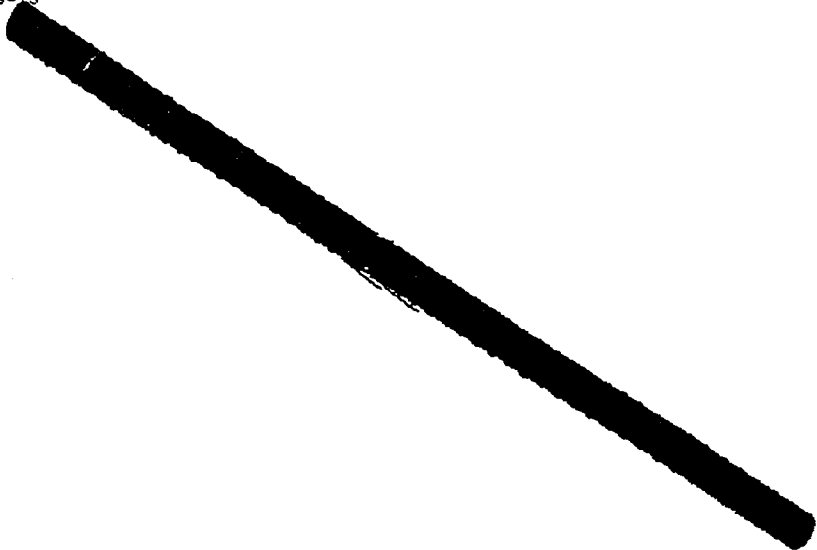
Hz



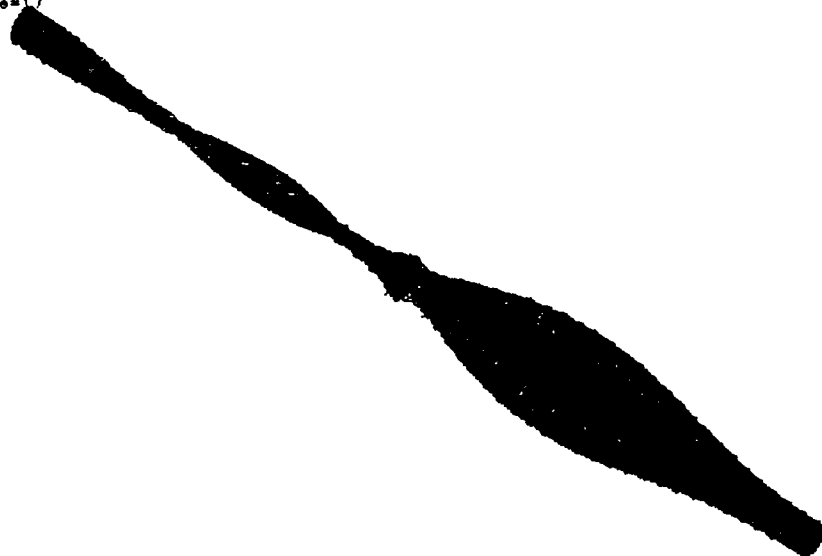
45 Hz F_Mode=13



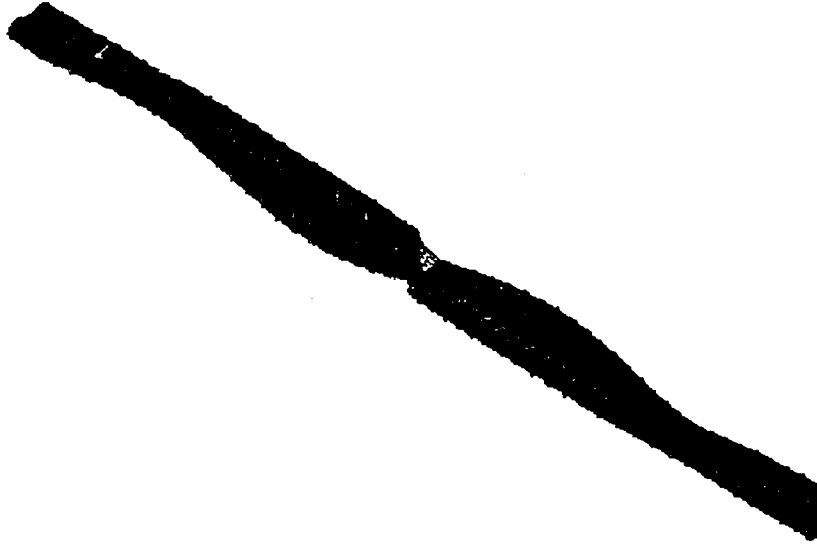
52 Hz F_Mode=15



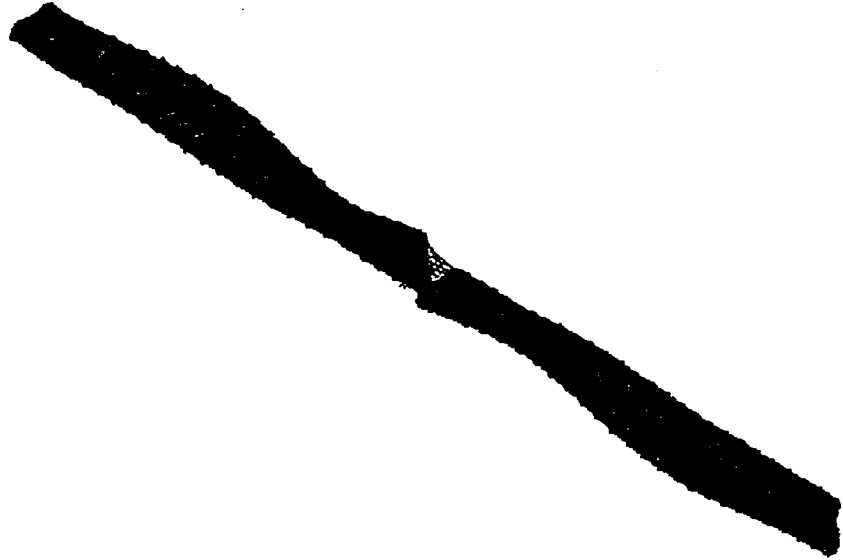
55 Hz F_Mode=17



55 Hz F_Mode=19



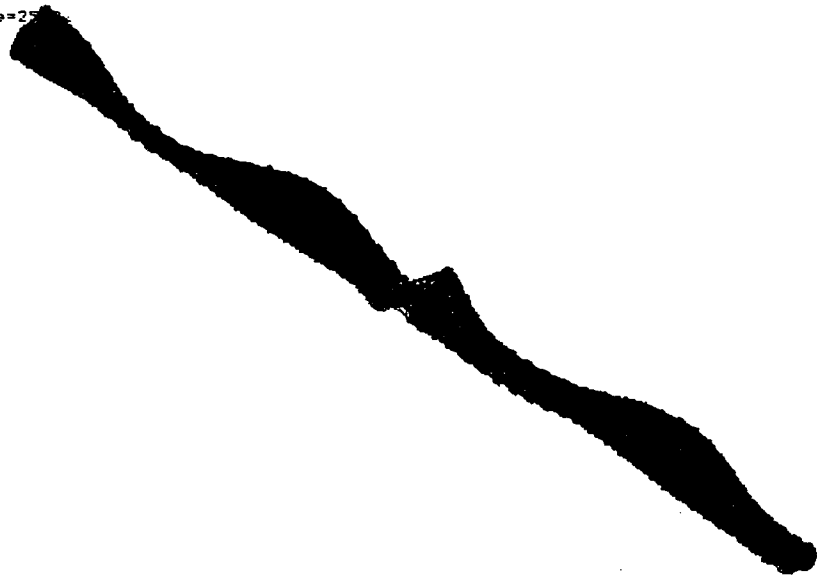
55 Hz F_Mode=21



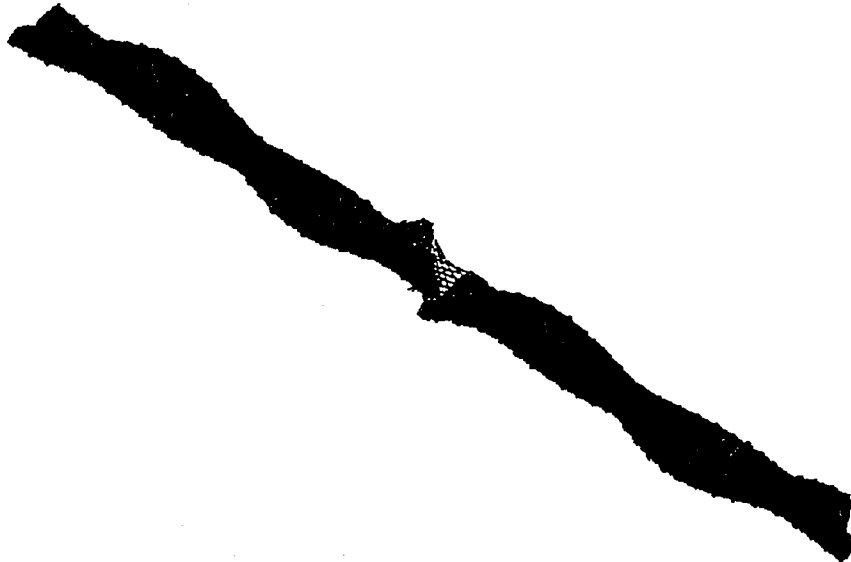
55 Hz F_Mode=28



58 Hz F_Mode=25



58 Hz F_Mode=27



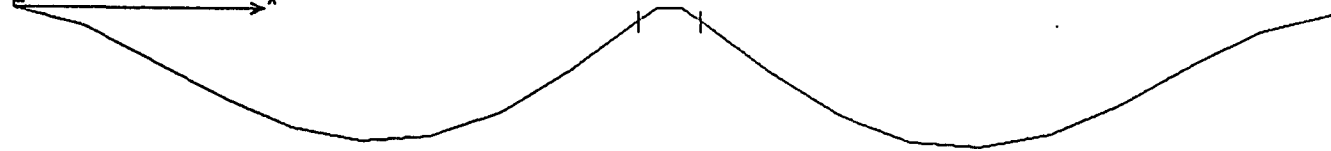
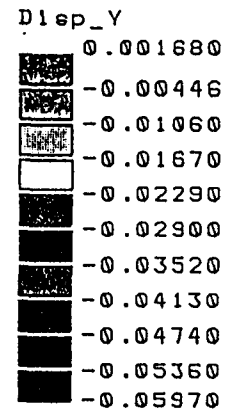
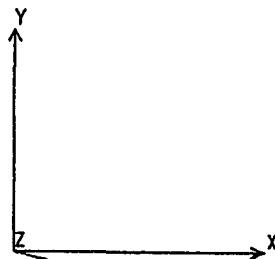
3D Beam Model

Static, Gravity-Induced Displacement

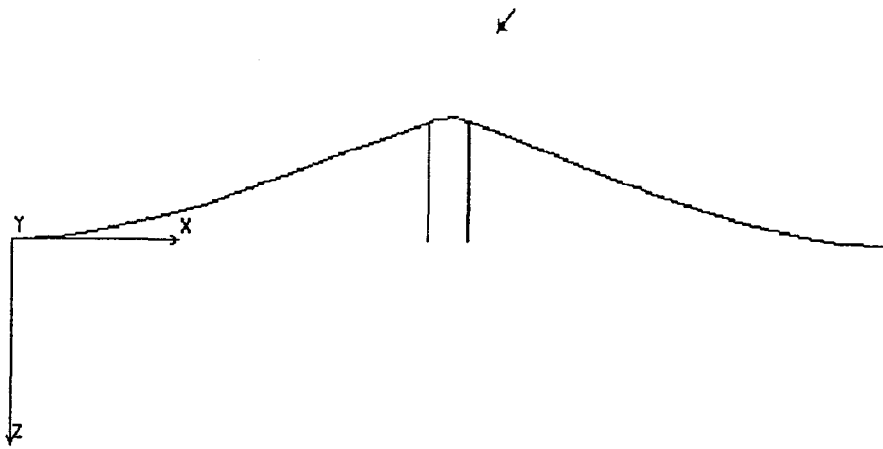
Natural Frequencies of Vibration

Deformed Mode Shapes

Lin DISP Lc=1



F_Mode=1 3.1 Hz



F_Mode=1 3.1 Hz

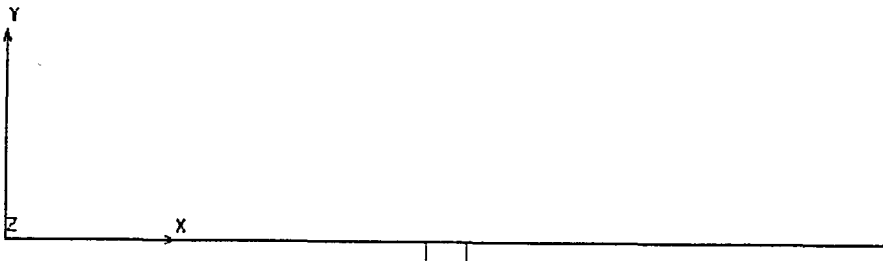
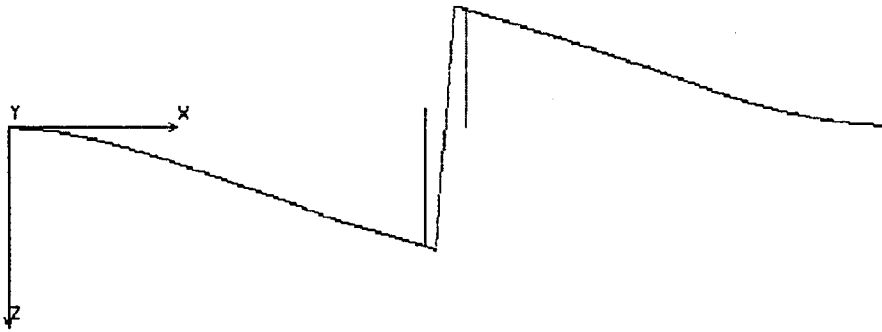


Figure 1: Mode 1, 3-D Beam Model Insulation Included

F_Mode=2 5.3 Hz



F_Mode=2 5.3 Hz

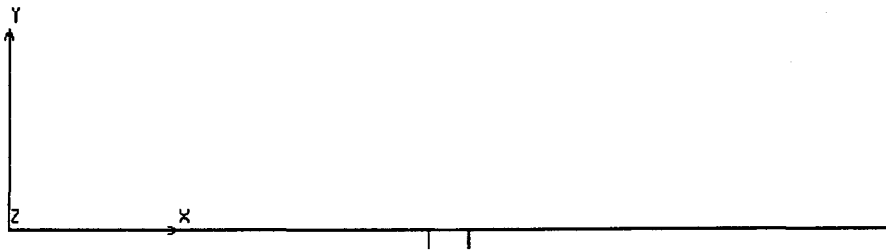
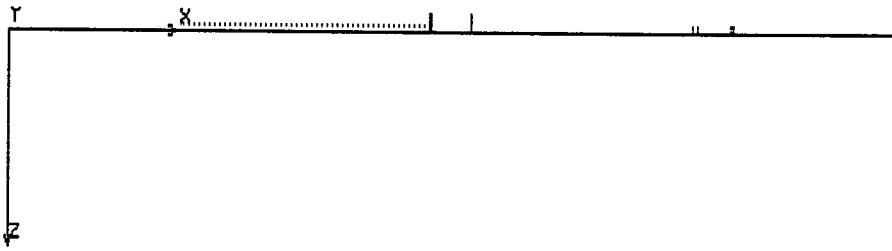


Figure 2: Mode 2, 3-D Beam Model Insulation Included

F_Mode=3 13 Hz



M₃₁



F_Mode=3 13 Hz

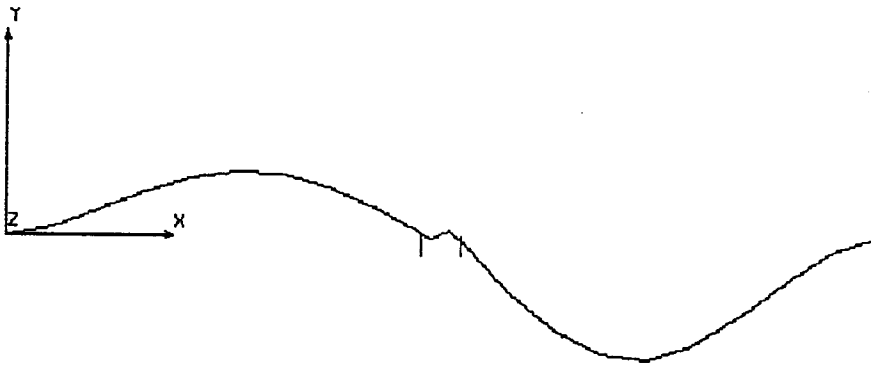
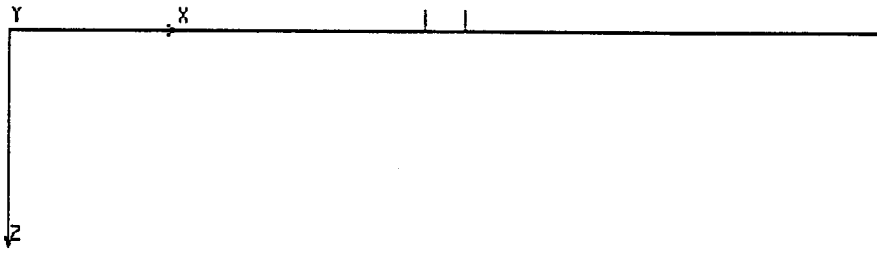


Figure 3: Mode 3, 3-D Beam Model Insulation Included

F_Mode=4 13 Hz



F_Mode=4 13 Hz

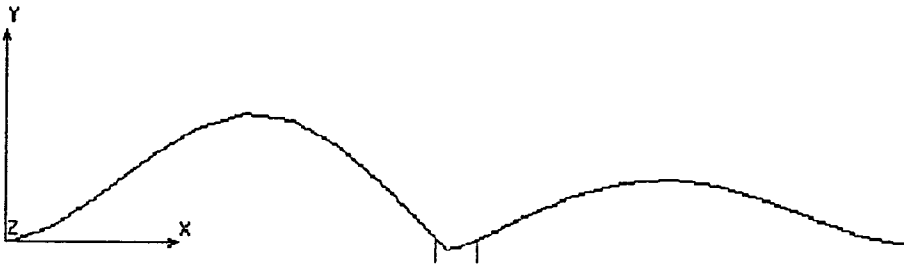
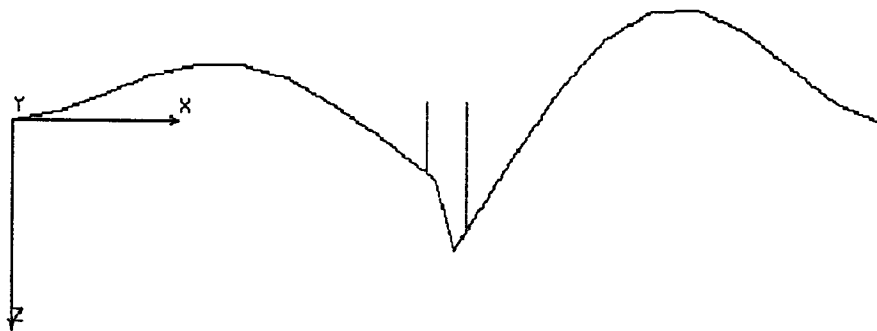


Figure 4: Mode 4, 3-D Beam Model Insulation Included

F_Mode=5 17 Hz



F_Mode=5 17 Hz

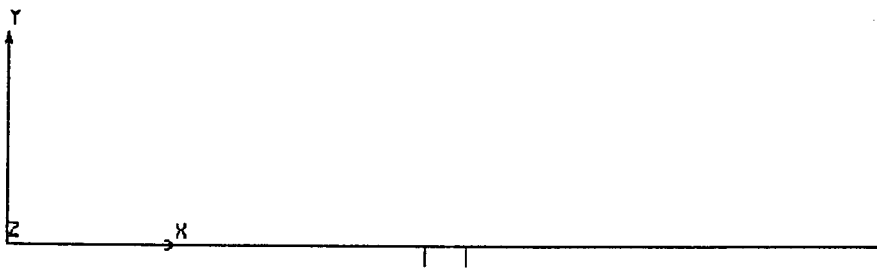


Figure 5: Mode 5, 3-D Beam Model Insulation Included

F_Mode=6 17 Hz



F_Mode=6 17 Hz

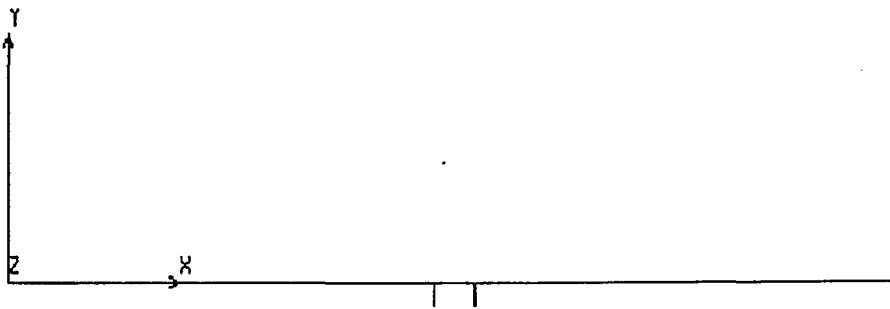
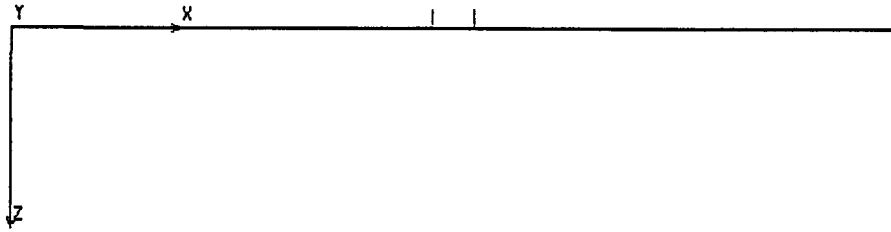


Figure 6: Mode 6, 3-D Beam Model Insulation Included

F_Mode=7 39 Hz

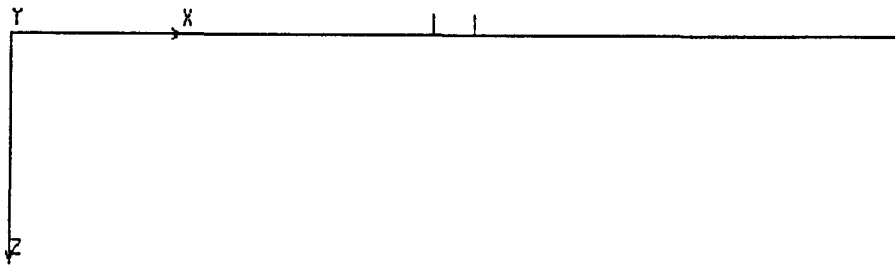


F_Mode=7 39 Hz



Figure 7: Mode 7, 3-D Beam Model Insulation Included

F_Mode=8 39 Hz

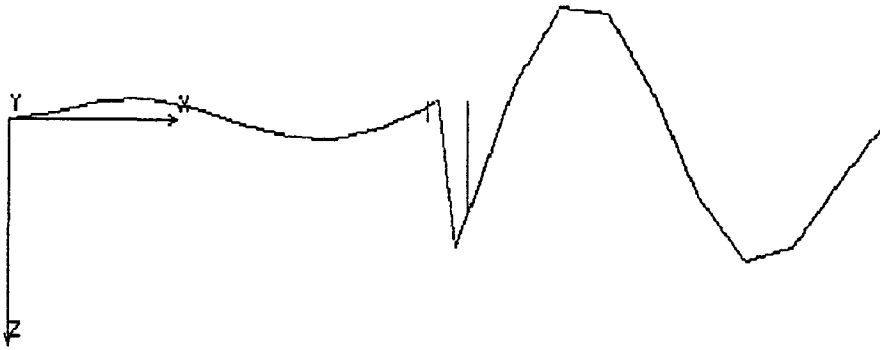


F_Mode=8 39 Hz



Figure 8: Mode 8, 3-D Beam Model Insulation Included

F_Mode=9 44 Hz



F_Mode=9 44 Hz

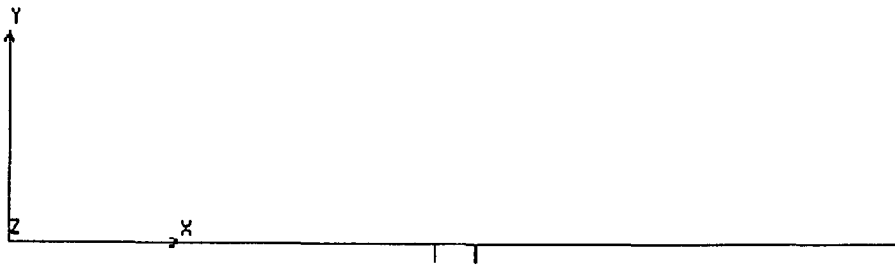
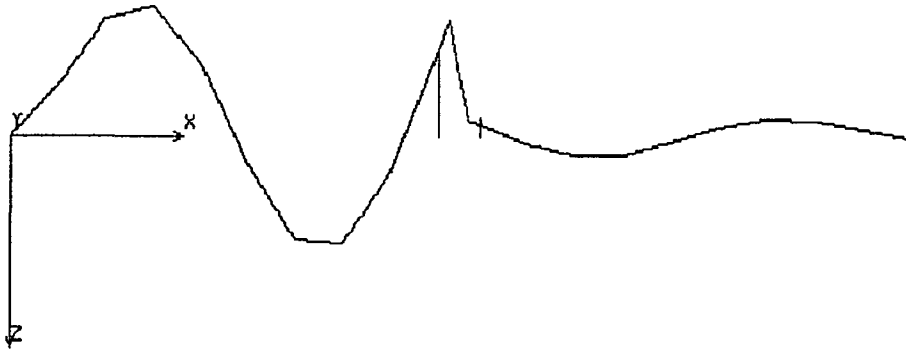


Figure 9: Mode 9, 3-D Beam Model Insulation Included

F_Mode=10 44 Hz

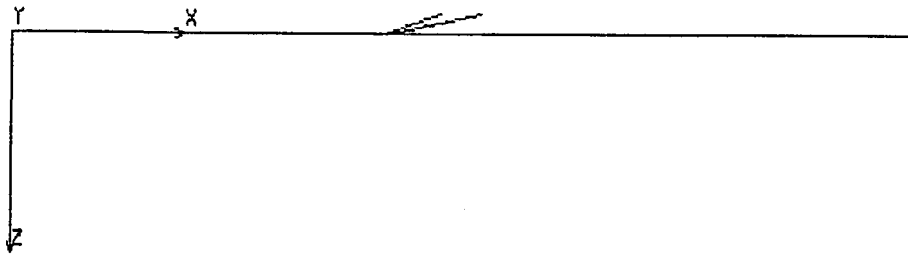


F_Mode=10 44 Hz



Figure 10: Mode 10, 3-D Beam Model Insulation Included

F_Mode=11 55 Hz

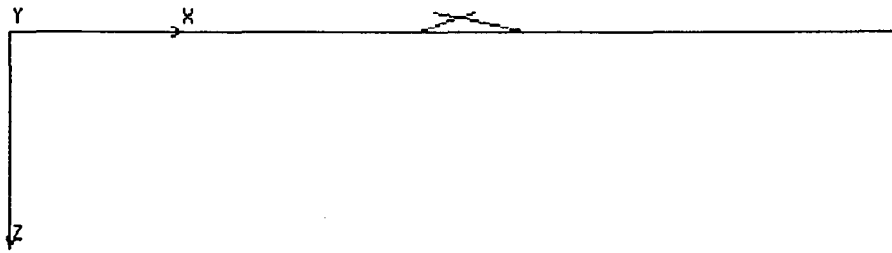


F_Mode=11 55 Hz



Figure 11: Mode 11, 3-D Beam Model Insulation Included

F_Mode=12 56 Hz

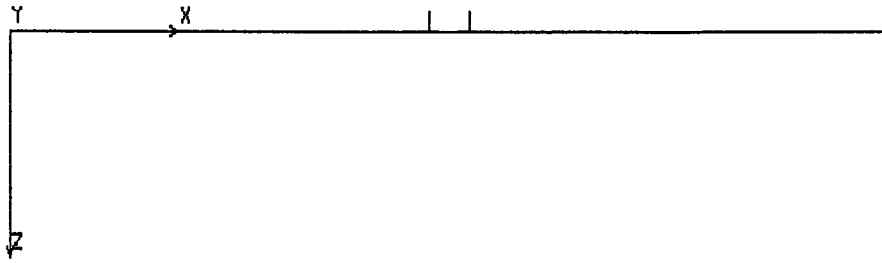


F_Mode=12 56 Hz



Figure 12: Mode 12, 3-D Beam Model Insulation Included

F_Mode=13 68 Hz



F_Mode=13 68 Hz

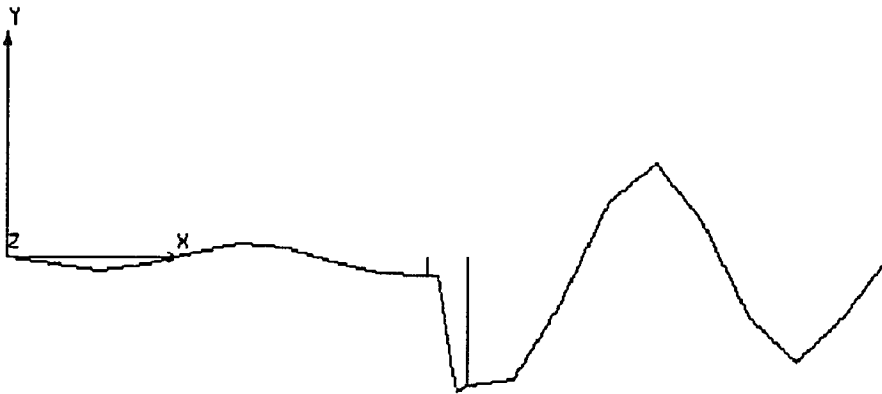
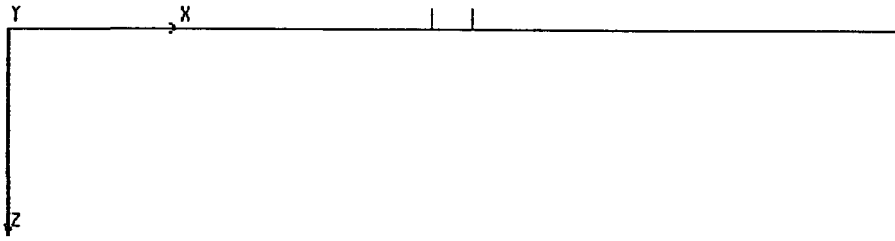


Figure 13: Mode 13, 3-D Beam Model Insulation Included

F_Mode=14 69 Hz



F_Mode=14 69 Hz

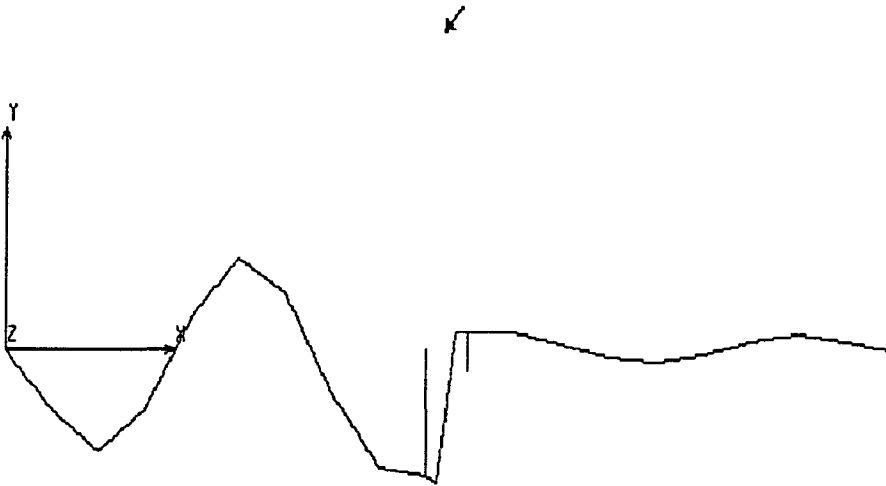


Figure 14: Mode 14, 3-D Beam Model Insulation Included

F_Mode=15 80 Hz



F_Mode=15 80 Hz

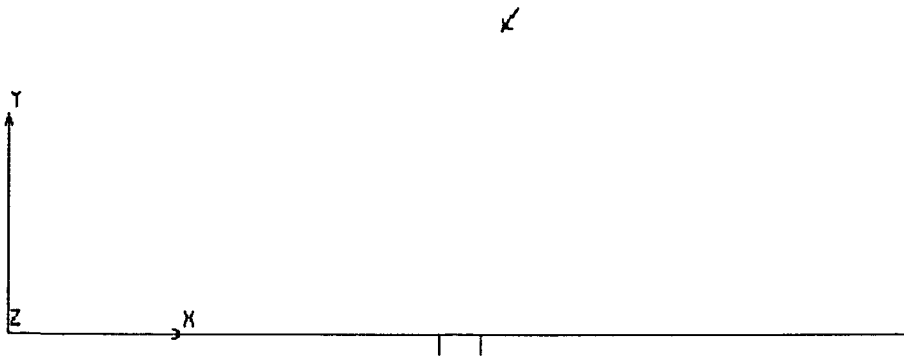
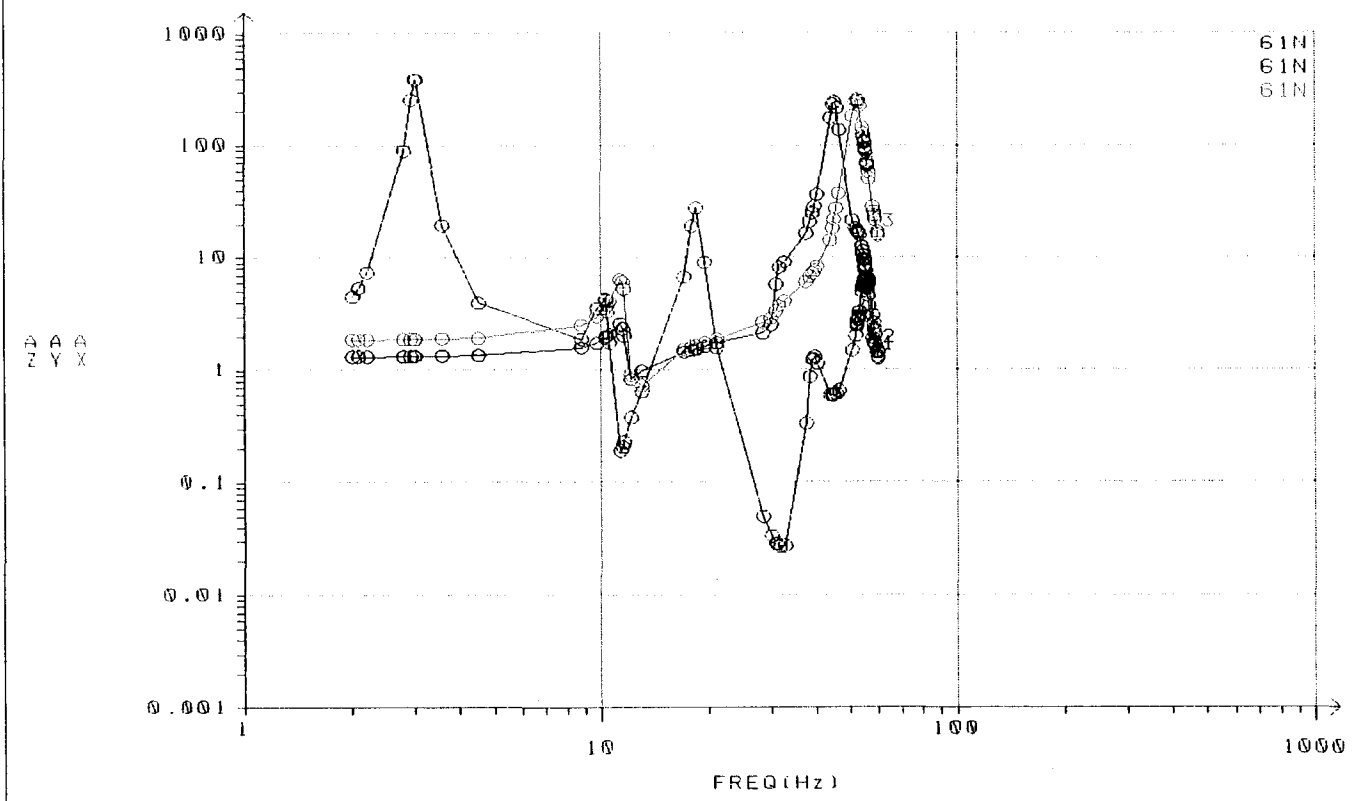


Figure 15: Mode 15 3-D Beam Model Insulation Included

3D Shell Model

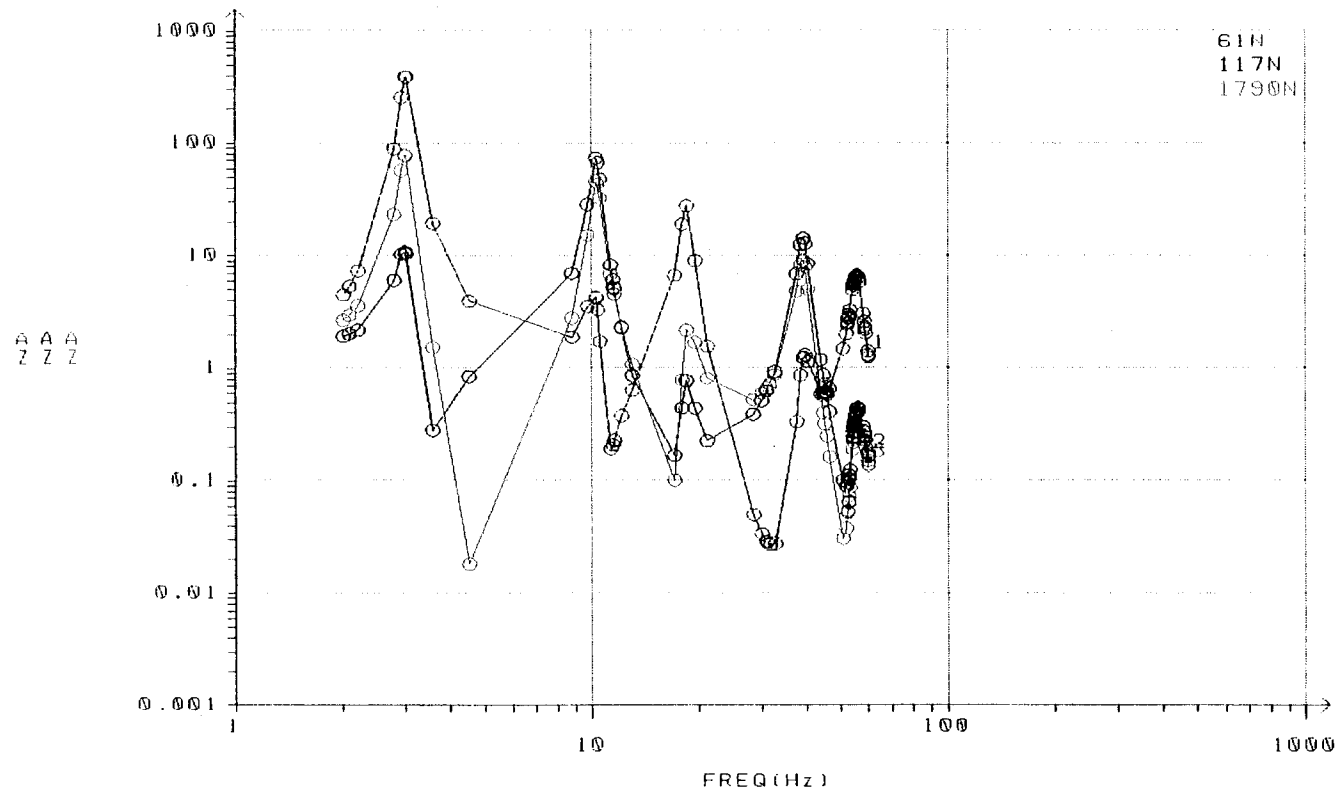
Transfer Functions $|H(f)|^2$
With Insulation Weight
4% Modal Damping

Acceleration PSD=1
 4% Modal Damping Shell Model



Node 61 @ x=762
 Similar to node
 12 in 3-D Beam Soln

Acceleration PSD=1
4% Modal Damping Shell Model

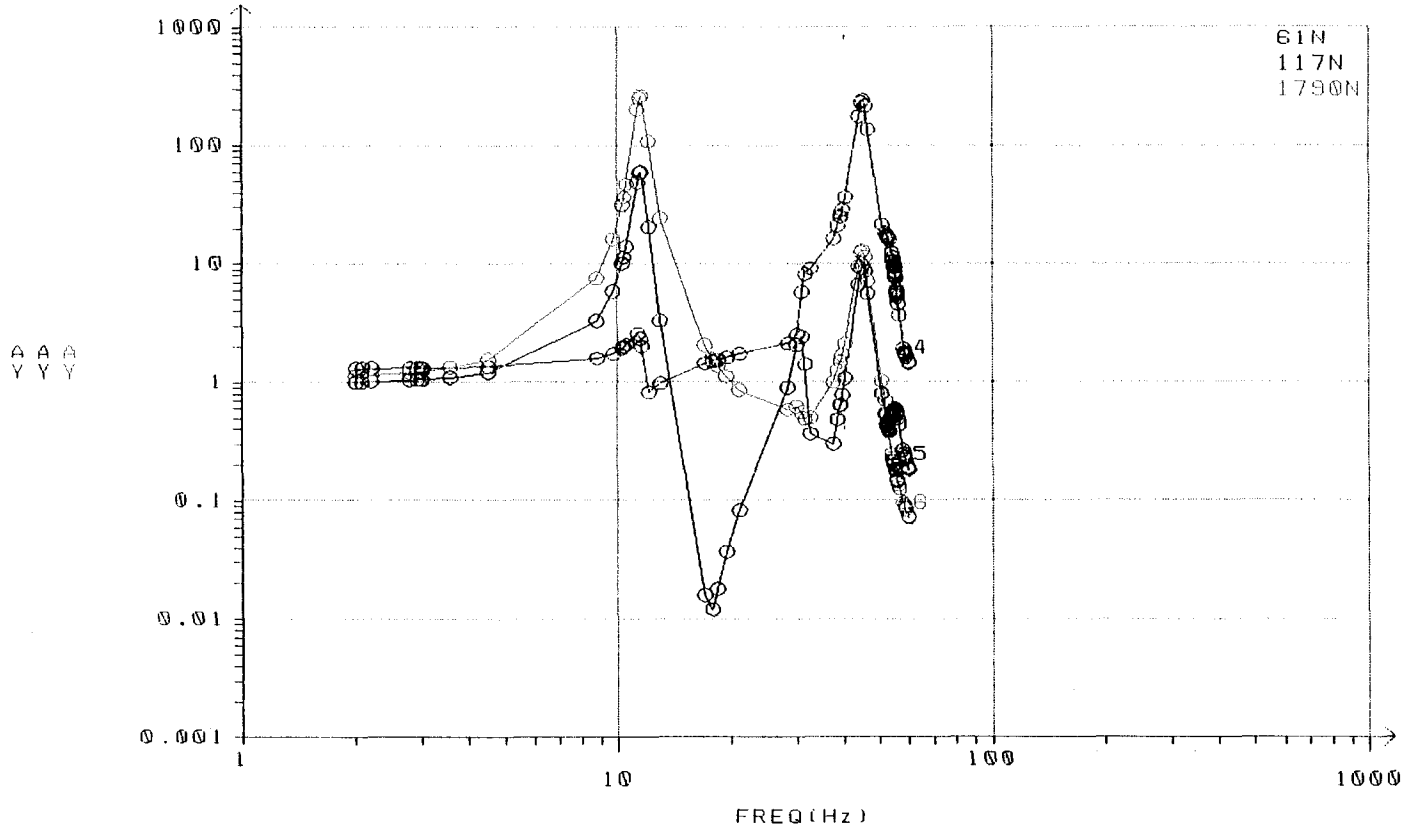


Node 61 @ X=76Z
Similar to node
12 in 3-D Beam Soln

Node 117 @ X=170.8
Similar to node 3
in 3-D Beam Soln

Node 1790 @ X=1140
Similar to node 19
in 3-D Beam Soln

Acceleration PSD=1
 4% Modal Damping Shell Model



Node 61 @ X=762
 Similar to Node
 12 in 3-D Beam Soln

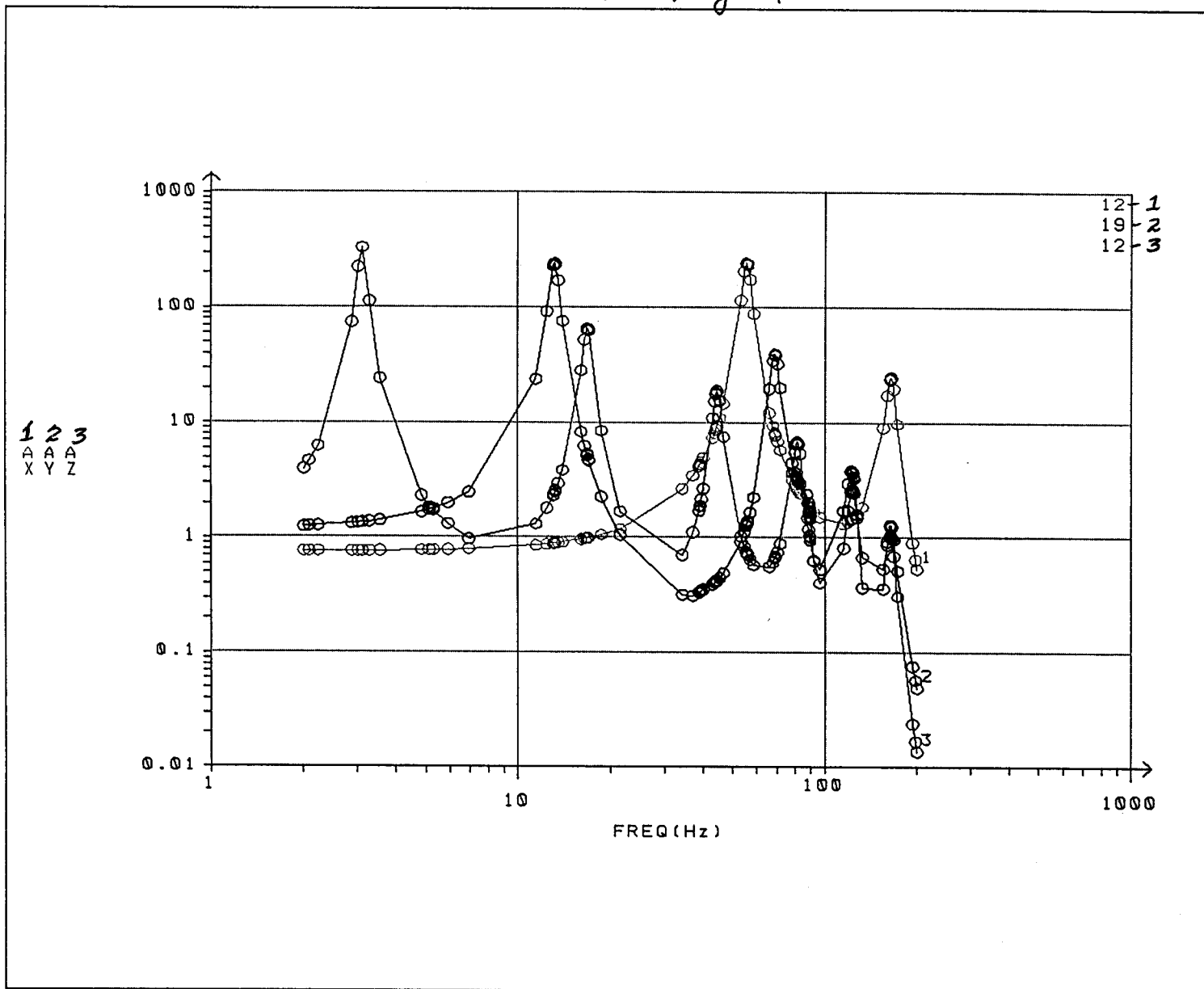
Node 117 @ X=171
 Similar to Node
 3 in 3-D Beam Soln

Node 1790 @ X=1140
 Similar to Node
 19 in 3-D Beam Soln

3D Beam Model

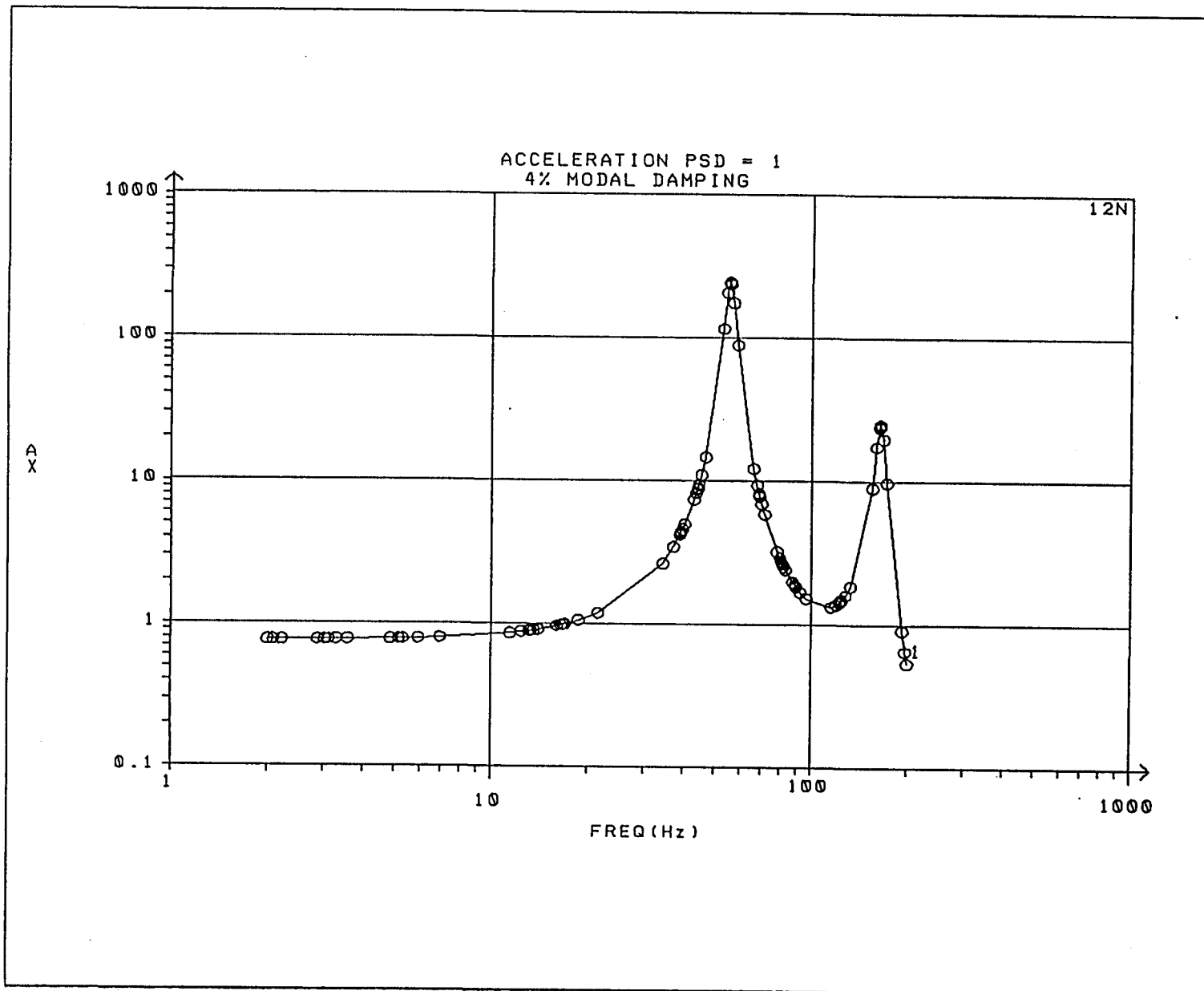
Transfer Functions $|H(f)|^2$
With Insulation Weight
2% Modal Damping

3D Beam Model
 Unit Accel PSD Input
 4% DAMPING w/ Insulation



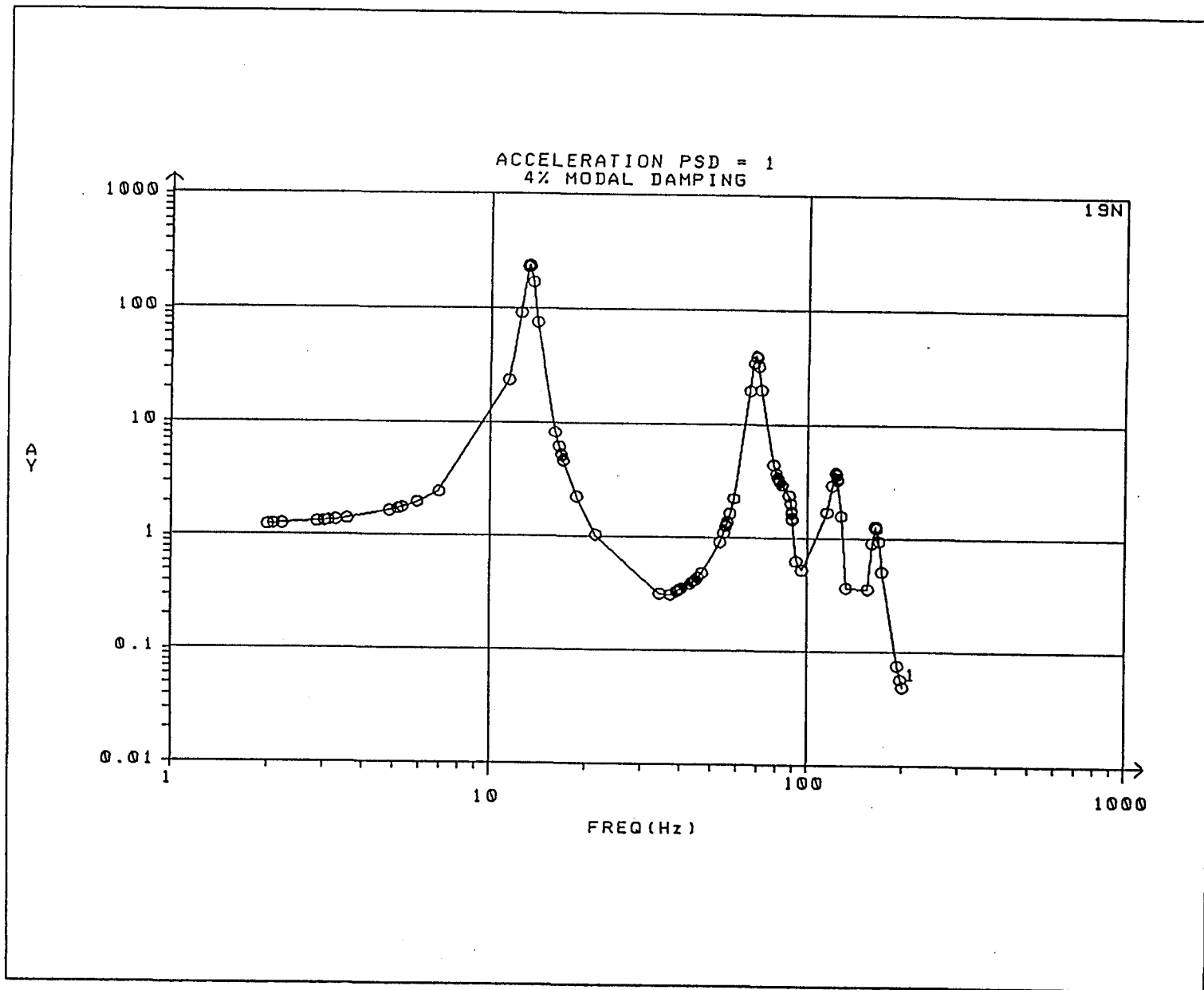
Units - $\frac{(\frac{\mu m}{s^2})}{Hz}$

Date: 2/25/96
 Fig: 13
 Page: 22



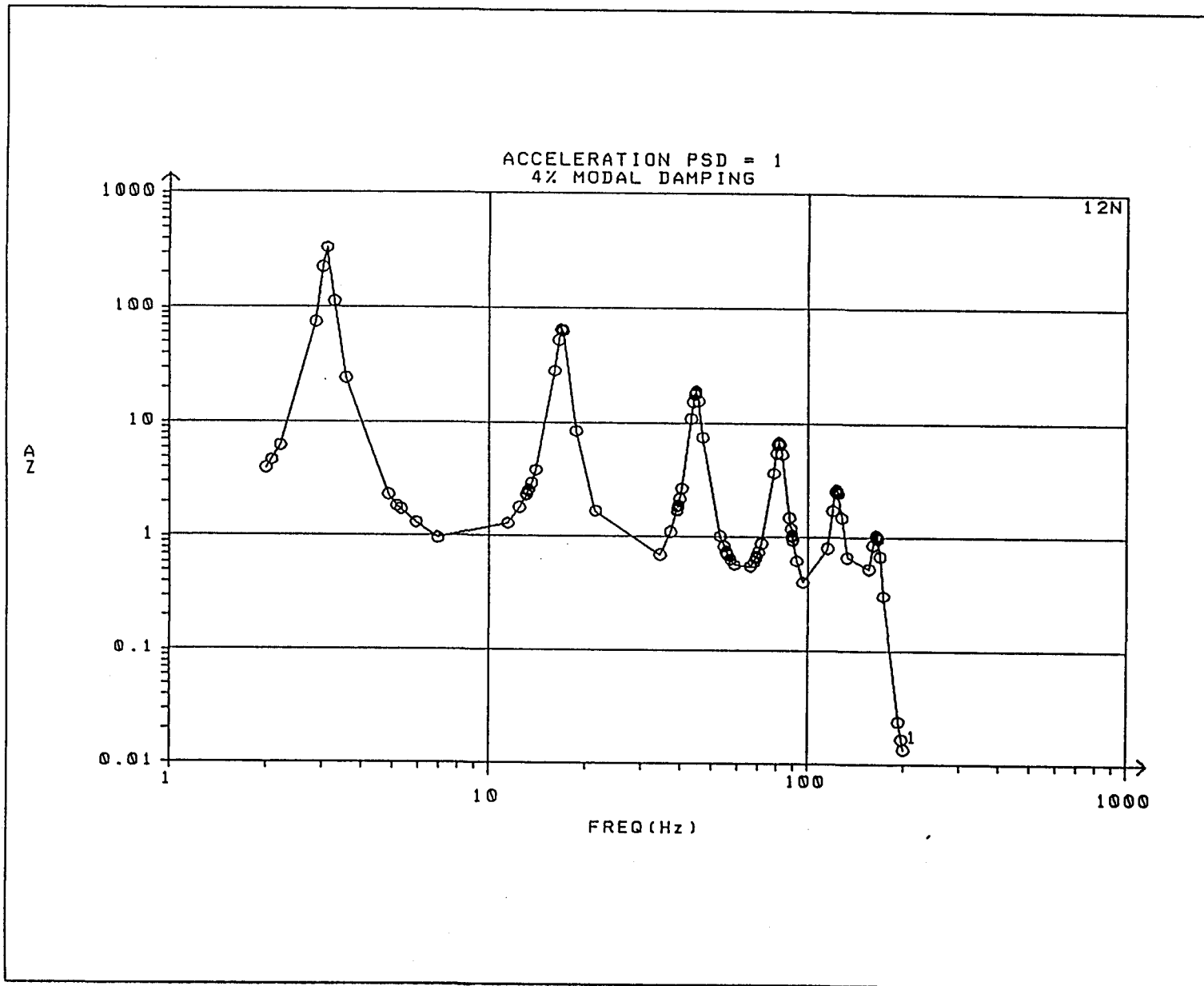
Units - $A_x \frac{(\frac{\mu\text{in}}{\text{s}^2})^2}{\text{Hz}}$

Date: 2/25/95
Fig: 10
Page: 18



Units - $A_y \frac{(\mu\text{in})}{\text{SL}}$

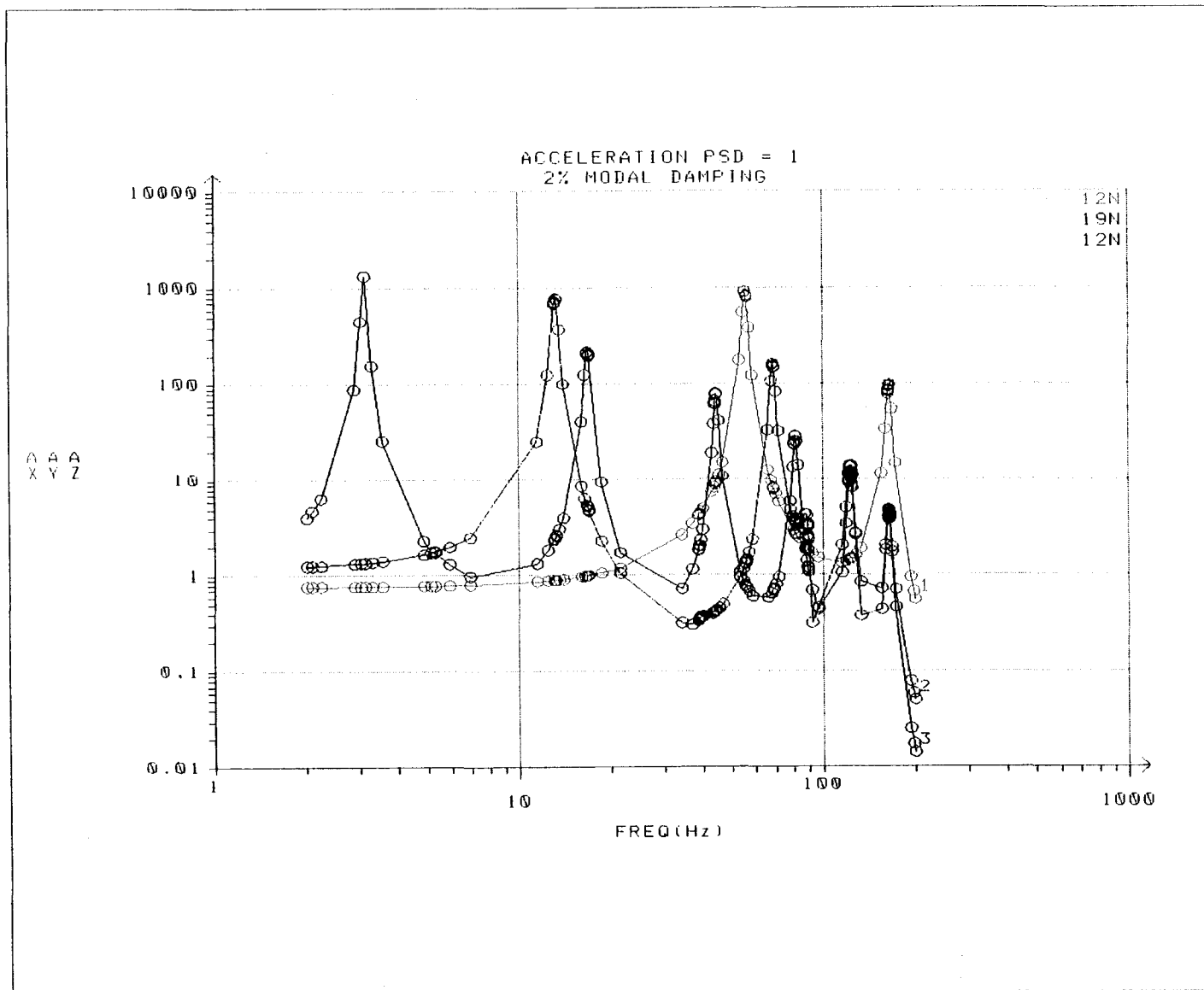
Date: 2/25/95
Fig: 11
2 0 0 0

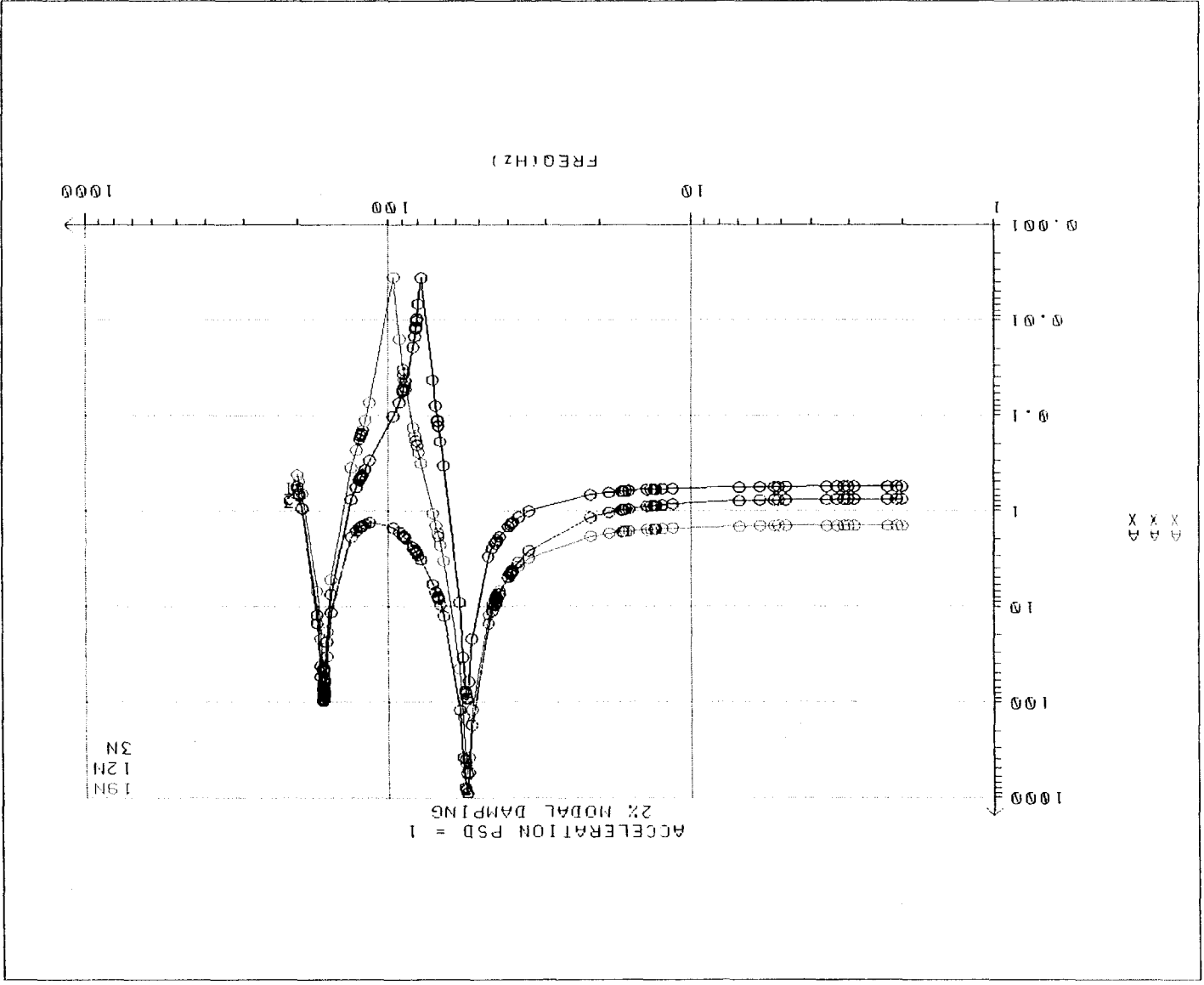


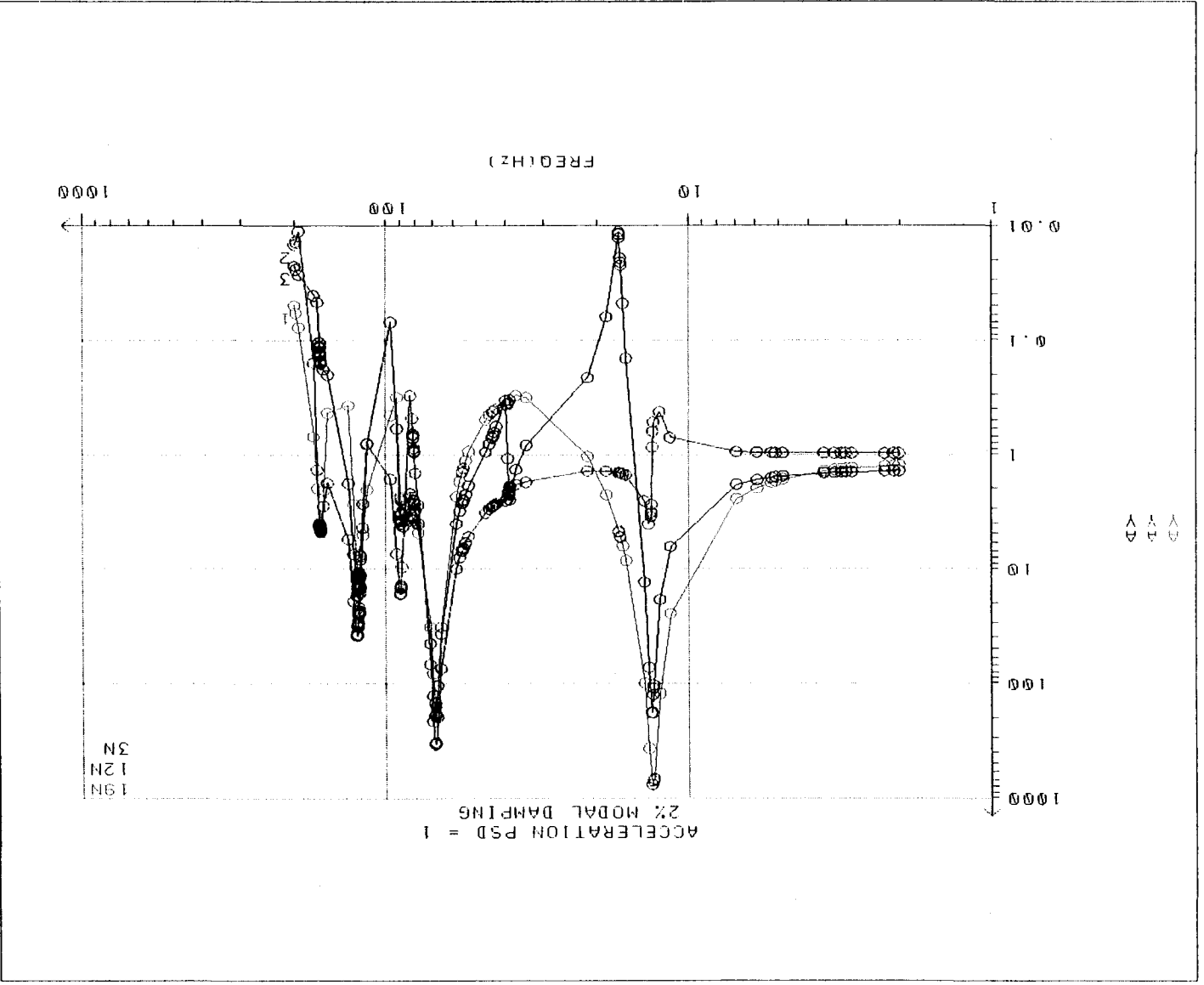
Date: 2/25/95
Fig: 12
①

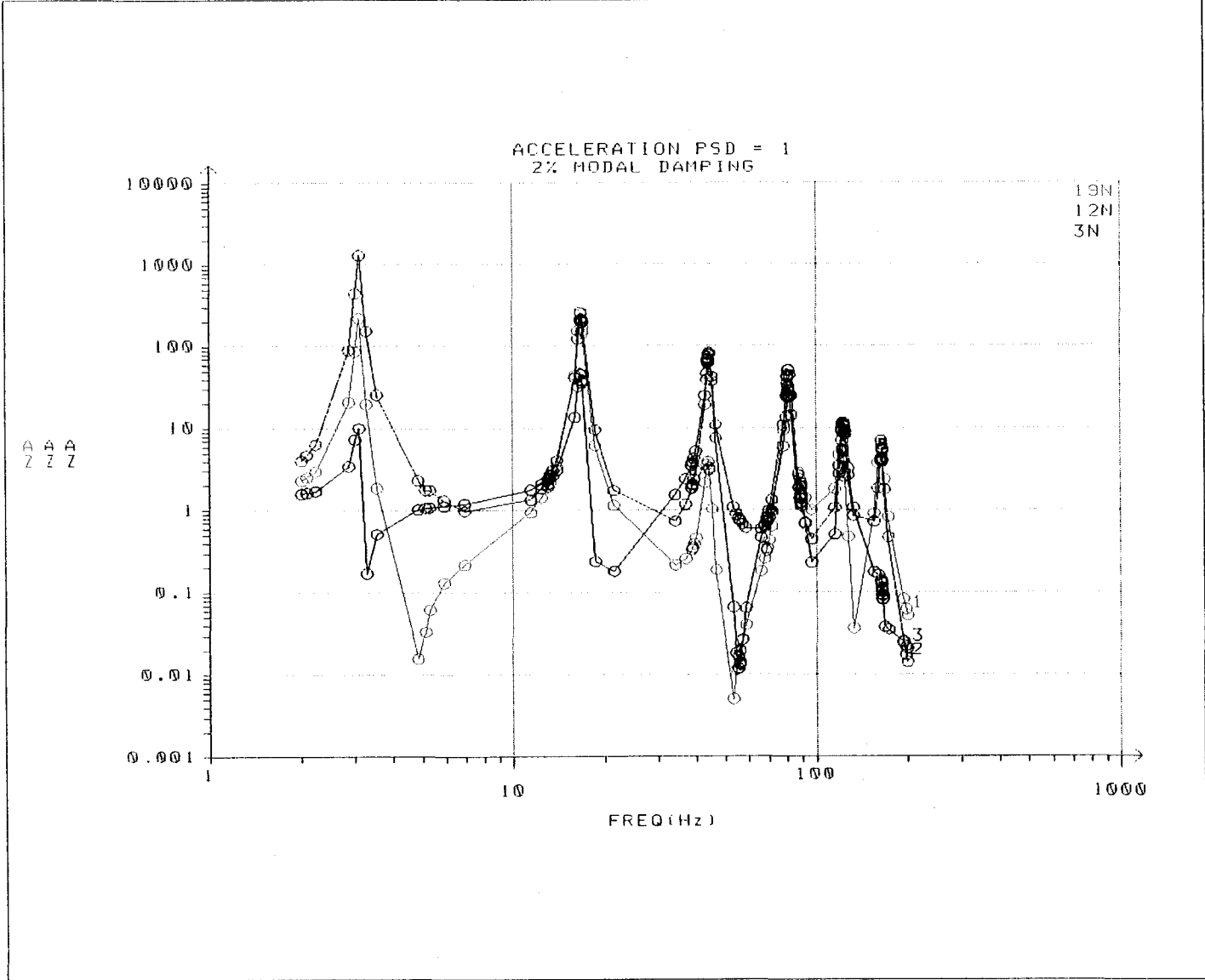
3D Beam Model

Transfer Functions $|H(f)|^2$
With Insulation Weight
2% Modal Damping



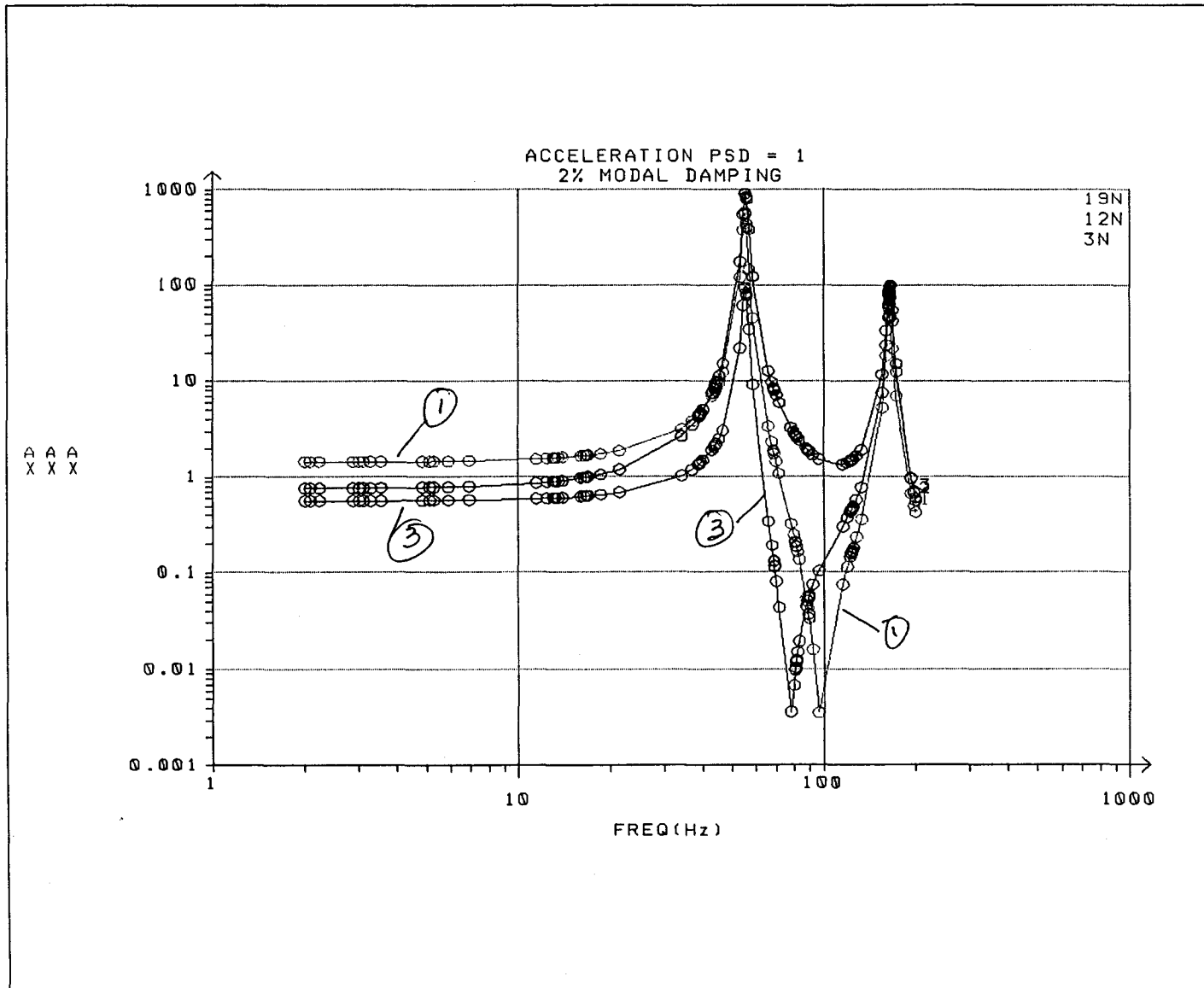


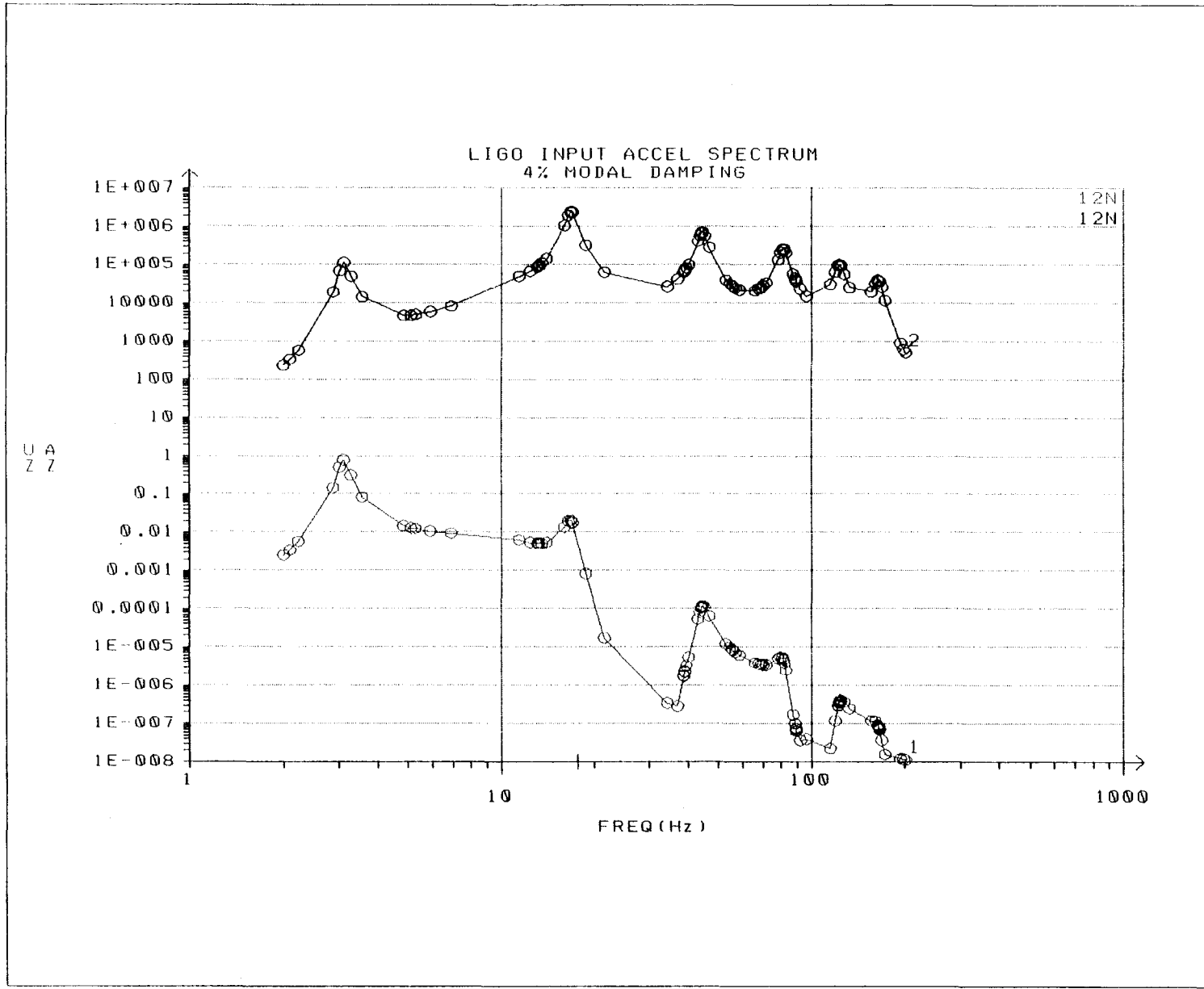




3D Beam Model

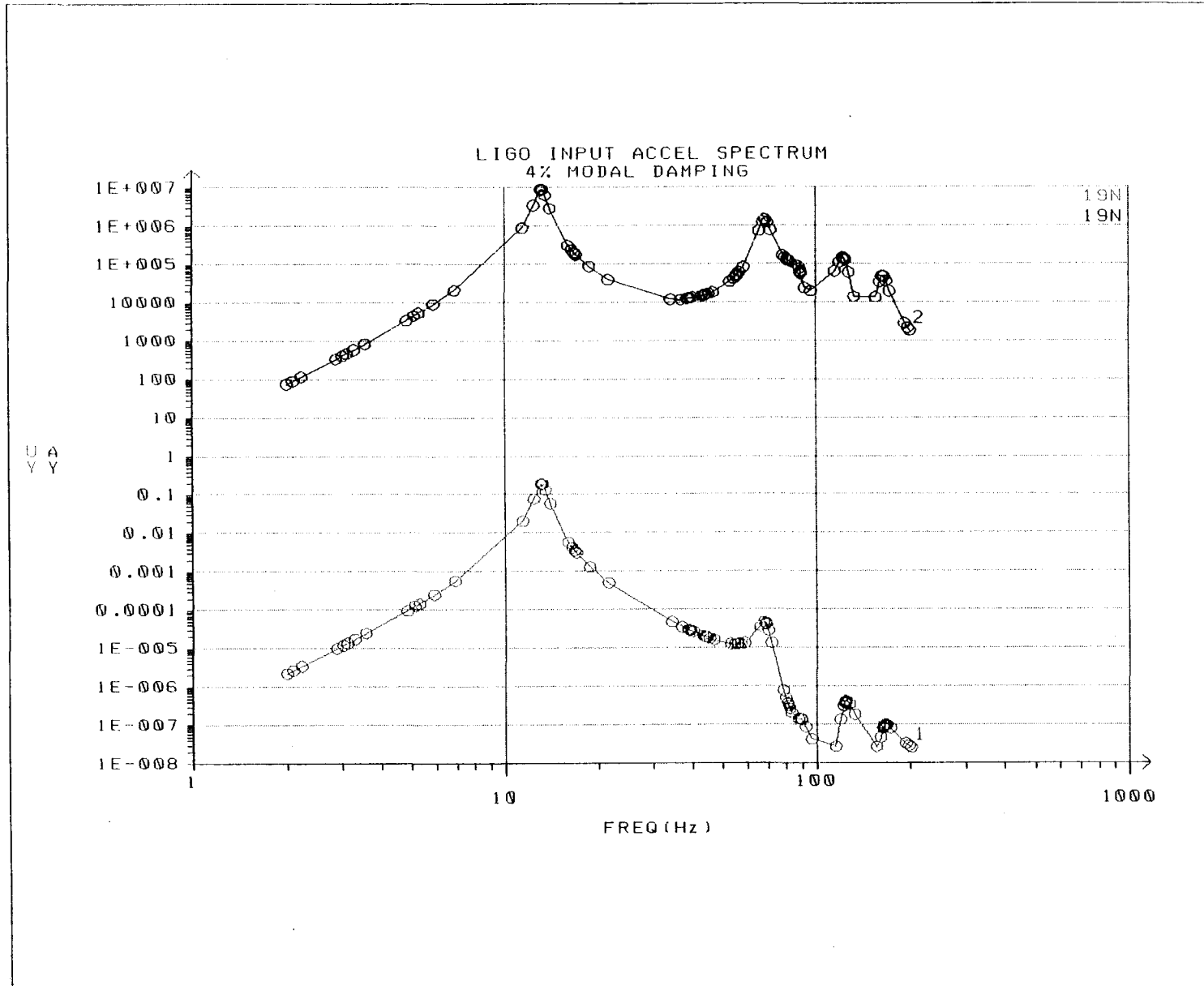
Response to LIGO Input Power Spectrum
With Insulation Weight
4% Modal Damping
Units are (micro-inches)²/Hz !





Units - $A_z \left(\frac{\mu m}{s^2} \right)^2$

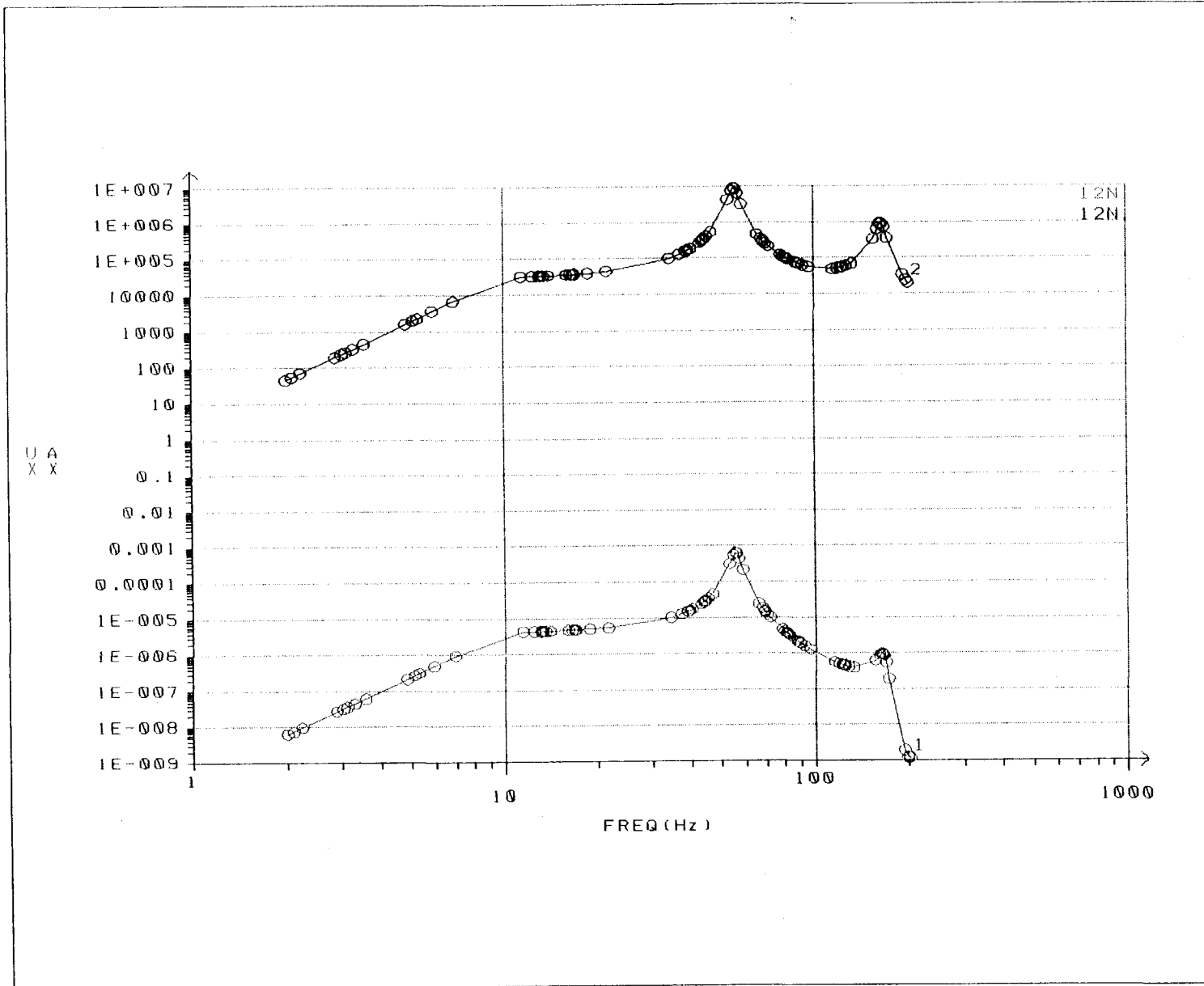
Date: 2/25/05
Figure: 5
Page: 9



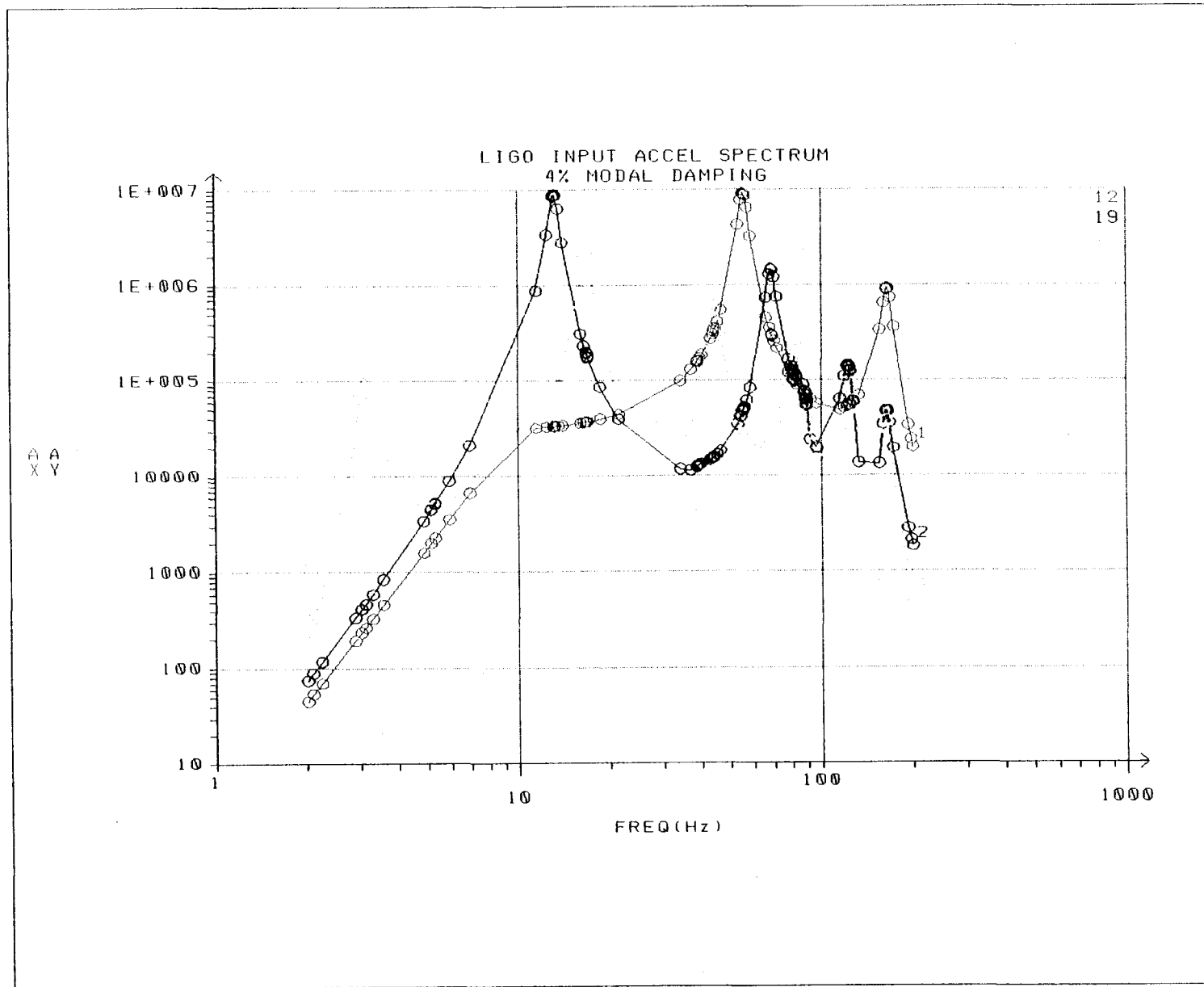
Units - $A_y \left(\frac{\mu\text{m}}{\text{s}^2} \right)^2$ $U_y \left(\frac{\mu\text{m}}{\text{s}^2} \right)^2$

Date: 2/25/95
Figure: 4
Page: 7

LIGO Input Accel Spectrum
4% Modal Damping



Units - $A_x \frac{(\text{Min})^2}{\text{Hz}}$ $U_x \frac{(\text{Min})^2}{\text{Hz}}$



Date: 2/25/95
 Fig: 9
 Page: 17